Dear Editor,

We appreciated the careful assessment of our manuscript by three highly qualified reviewers and were very pleased by the positive and constructive comments they provided. The reviewers made some useful suggestions to strengthen the manuscript, which we have addressed in the revised manuscript. Below, we provide our responses to the comments raised by reviewers (individually uploaded on the interactive discussion), the revised manuscript and the supplementary information. We highlighted the changes made in response to the reviewers in yellow.

We have also further marked some changes unrelated to the reviewer's comments in green . We now discuss the new IPCC recommendations published by Requena Suarez et al. 2019 during the review process of our manuscript. These new recommendations lead to a decrease by half of the default rate of carbon accumulation in Asian tropical secondary rainforests but was based on very limited data. Because our results do not support these updated rates, we believe that this discussion will attract many readers. Also, some minor mistakes, unrelated to referee's comments, were corrected in red in the revised manuscript.

Finally, the removal of second affiliation of the first author was done to meet the university guidelines towards doctoral publication.

We hope that the corrected manuscript is now suitable for publication in *Biogeosciences*.

Thank you for your time and consideration.

Sincerely yours,

On behalf of the authors,

Nidhi Jha

Response to the comments by Anonymous Referee #1 on "Forest aboveground biomass stock and resilience in a tropical landscape of Thailand"

Dear Reviewer,

Thank you for the careful and attentive assessment of our manuscript. We are very pleased with the positive and constructive comments provided for our work. Please find below our point-by-point response to your *italicized* comments.

On behalf of the authors,

Nidhi Jha

Reviewer #1: *This is a robust and well-written study that combines field measurements, multitemporal satellite imagery, and airborne laser scanning data at the landscape scale to estimate rates of biomass accumulation in naturally regenerating forest vegetation in Khao Yai National Park in central Thailand. As such high-quality information is lacking from most regions of Asia, this study will be a landmark case and illustrates how combinations of different data sources can be used to track changes in landscape scale biomass accumulation and carbon storage in the absence of long-term monitoring data from forest sites. I applaud the authors on a job well done.*

Response: Thank you.

Reviewer #1, C1: *One shortcoming of their model is that very few field sites had low ABG values, so the model may not be as accurate at predicting AGB at low levels.*

Response: We agree with the reviewer that we do have a limited number of field plots in low-biomass areas. That said, we do not believe that this constitutes a major problem as model uncertainty is expected to be higher for large biomass values than for small biomass values (Zolkos et al. 2013, Remote Sensing of Environment), as suggested by Fig. 2 of our manuscript. Thus, getting a higher representativity of large AGB values in the model is recommended to minimize model calibration errors.

However, we followed the recommendation of Reviewers 1 and 2 and added the following sentence in section 4.1 in revised manuscript.

"Due to a limited number of field plots in low-biomass areas we were, however, unable to test whether predicting errors vary with AGB or not."

Reviewer #1, C2: *With the data that they have, the authors estimated the distribution of AGB values across the landscape. These data were used to estimate mean landscape-scale AGB (and carbon density) for 2017. With the information on changing states of pixels from non-forest to forest (or from forest to non-forest), it should be possible to estimate how the distribution, mean,* *and total AGB within the landscape changed from the mid-1970s to the present day. This would be fascinating to do (if not in this paper, then in another one).*

Response: We agree that tracking the AGB distribution over time would be extremely informative and would provide important insights on the carbon balance of the landscape. However, we here face one important limit of our approach that prevent us to assess the landscape scale carbon balance over the study period. Our approach only allows to assess the AGB dynamics of pixels that experienced a single shift from non-forest to forest during the study period. Although this approach generates much more data than usually available through field-based approaches (n=550 in our case), these pixels only represent 4% of the landscape and are thus not representative of the whole landscape carbon dynamics. In an ongoing work, we are adopting another approach where we use field estimates of carbon dynamics and extrapolate them through a LiDAR-based forest successional map to estimate the carbon balance of the landscape. Thus, this objective will be rather achieved in another upcoming paper.

Additional comments:

Reviewer #1, C3: *Line 36-38: this statement does not describe what Chazdon et al. 2016 concluded. They found that 40 yr of carbon storage in regenerating forests of lowland regions of Latin American tropics alone offset the past 19 years of carbon emissions from fossil fuel burning and industrial sources from all of Latin America (not total carbon emissions).*

Response: We agree with the comment and thank the reviewer for pointing this mistake. We rephrased this statement in the revised manuscript as following:

"A previous study estimated that 40 years of carbon storage in regenerating tropical forests from Latin America offset the past 19 years of carbon emissionsfrom fossil fuels and industrial production at the scale of Latin America (Chazdon et al., 2016)."

Reviewer #1, *C4: Line 102: what is the age and prior land use of this secondary forest?*

Response: This area is a regenerating successional forest resulting from farming activities (mostly rice cultivation) that stopped in the 1960s. Our analyses suggest that these areas shifted from a non-forest to a forest status in 1975 (see SES4 and SES5 in Fig. S4 of original manuscript, now Fig S5 in revised manuscript).

Reviewer #1,C5*: Line 112: were there any stands in the understory initiation phase? Some details from Chanthorn et al. 2017 should be included here*

Response: None of the plots are in the understory re-initiation stage. To make it clear we added the following information in the revised manuscript after L112 of original manuscript.

"The classification is based on the framework of Oliver and Larson (1996) who studied successional gradients in temperate forests. Although the original framework considered four

successional stages, we did not find any area corresponding to the understory re-initiation stage in the study landscape. Most second-growth forests have regenerated since the Park was established about 40-50 years ago so that older second-growth forests, where understory re-initiation occurs, is very rare in this area. In our study, the SES stage is represented by forest of upto 35-40 years, while other SES area in the landscape may typically range upto 55 years (since 1962), as suggested by some hand drawn historic maps (Smitinand, 1968; Cumberlege & Cumberlege, 1964). On the other hand, OGS forest stands mostly correspond to forests with no obvious sign of human disturbance during the last 100 years (Brockelman, 2011).”

Reviewer #1,C6: *Line 155: but only those > 5 cm dbh, right?*

Response: Yes, correct. For sake of clarity we modified the sentence in the revised manuscript as following:

“AGB at the plot level was then estimated in Mg ha^{-1} by summing individual tree AGB for all trees with dbh ≥ 5cm belonging to the plot.”

Reviewer #1,C7: *Line 241: I would take out the word "probably" Why wouldn’t it? How has the carbon storage in the landscape changed over time? That would be great to show, not just for 2017 (would just need to assess these changes for the 17% of pixels that showed changes and keep the same AGB figures for the remaining 83% of the pixels). This projection would be nice to include in the final version of the manuscript.*

Response: Please, see our response to comment C2. Keeping the same AGB values for the 83% pixels would lead to a strong underestimation of the carbon sink in this landscape, as revealed by our ongoing work. We, however, removed the word probably in the Line 241 and add the following sentence in section 3.2 in revised manuscript:

“Focusing on the 17% pixels that experienced at least one shift from non-forest to forest since 1972, we thus estimate that the study area has stored a minimum AGB of 455 Gg, equivalent to 214 GgC during the study period.”.

Reviewer #1,C8: *Line 270: The Poorter et al. 2016 study is based on trees > 10 cm DBH. This may explain some of the discrepancy. Can you evaluate the contribution of trees 5-10 cm DBH in the total stand ABG? May be useful for comparing results with other datasets from other regions.*

Response: Thank you for pointing this issue. According to our field data, the contribution of trees 5-10cm dbh to the total stand AGB ranges from 1% to 39% (average of 4.5%) and tend to decrease with successional stage. Thus, we indeed cannot exclude that part of the difference is due to the inclusion of trees of 5 to 10 cm in dbh. We have added the following sentence in revised manuscript to acknowledge this.

“After 20 years of recovery, our model predicts an AGB accumulation of 143 Mg ha−1, an estimate slightly higher than the one predicted by Poorter et al., (2016a) in Neotropical secondary forests (122 Mg ha−1). However, this difference can partly be explained by the inclusion of trees between 5 and 10 cm dbh in our study, contrary to Poorter et al. (2016)’s study.”

Response to the comments by Anonymous Referee #2 on "Forest aboveground biomass stock and resilience in a tropical landscape of Thailand"

Dear Reviewer,

We are thankful for your careful assessment and dedicated efforts towards improvement of our manuscript. We were very pleased to account for your positive and constructive comments. Please, find below our point-by-point response to your *italicized* comments.

On behalf of the authors,

Nidhi Jha

Reviewer #2: *This study combines field, airborne (Lidar) and satellite (Landsat) data to estimate biomass stocks and accumulation in a regenerating tropical forest in Thailand. The authors use multi-temporal Landsat images to identify and target pixels that went from "non forest" to "forest" since 1972. They estimate the rate of biomass gain of these pixels by regressing the recovering time and biomass estimations from a locally calibrated AGB model. Their approach is a clever and effective way to assess biomass dynamics in the absence of multi-temporal biomass maps, and will probably encourage similar future studies in other areas. Recovery from forest disturbance is an important but still poorly understood topic, and this study will definitely contribute to advancing this field. The paper is very well-written, clear and well organized. The methodology is on point and the authors use high quality validation methods, making the whole study very robust. All the methods used in this study have already been used in various studies, but the way the authors combine them is unique. The paper could be improved by making some minor changes presented below:*

Response: Thank you.

General comments:

Reviewer #2, C1: *My main concern is that only 3 plots with biomass <100Mg/Ha were used to make the AGB lidar model. This is an important point, since the study is focusing on low biomass/recovering areas. This should at the very least be addressed in the Discussion.*

Response C1: Please see our response to Reviewer #1 comment C1. As argued in our response, we agree that we have a rather limited number of low AGB value field plots, but we do believe that it did not much impact the LiDAR model. As said in the response to reviewer 1, we added the following sentence in section 4.1:

*"**Due to a limited number of field plots in low-biomass areas we were, however, unable to test whether predicting errors vary with AGB or not.**"*

Reviewer #2, C2: *Although I understand why the authors chose to focus on pixels that went from "non-forest" to "forest", I think it would be nice to also talk about the pixels that remained "non-forest". There is no information on these in the paper, as the authors are not making any distinction between the "non-changing" pixels (pixels that remained non-forest vs. pixels that remained forest). I think it would be very informative to see how much of the degraded pixels did not recover since 1972 (excluding roads). It would give a more complete picture of the state of the forest. Ignoring these pixels implies that all disturbed areas have recovered. It would be nice to mention this somewhere in the manuscript, and also perhaps making this distinction in Figure 4.*

Response C2: Thank you for this suggestion to which we agree. We thus highlighted areas that remained non-forested since 1972 in Figure 4 of the revised manuscript. About 5% of the study area stayed non-forested since 1972. Most of these areas correspond to areas that were continuously cleared by the Park for administrative or tourism purpose, such as building and camping areas, or wildlife watchpoints. We have added the distinction of the areas as follows which remained forested from all the non-changing pixels in the result section 3.2 in the revised manuscript.

"Figure 4a illustrates the resulting spatialized time series of non-forest-to-forest shifts over the study area and showed that most (83%) of the landscape did not experience such shift at 60-m resolution, out of which 5% of the area remained permanently non-forested over the 42-year study period. Most of these non-forested areas were continuously cleared and mostly correspond to National Park buildings, including tourist shops and guest houses or camping location"

Revised Figure 4

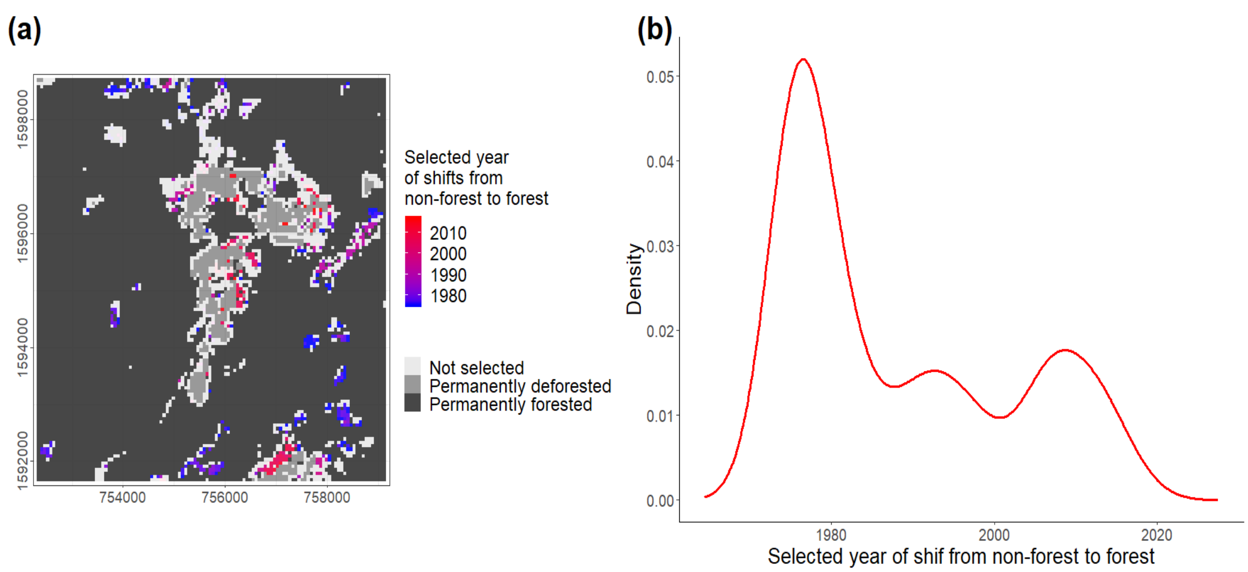

Specific comments:

Reviewer #2, C3: *L.89: How long before? Is there any historical information indicating when it started?*

Response C3: Unfortunately, we do have very limited information on the history of this area. The rough estimate of start of swidden agriculture is about the end of 19th century or early twentieth century (Chanthorn et al., 2016, Theoretical Ecology). For instance, Cumberlege & Cumberlege (1964, VMS Cumberlege Nat. Hist. Bull. Siam Soc 20), who studied orchids in Khao Yai National Park, mentioned that some secondary grassland patches in 1964 were the result of 80 years of swidden agriculture by villagers (hence starting around 1880). All villagers were then expelled by 1962 when the National Park was established (Chanthorn et al., 2017, Forest Ecology and Management). We briefly added estimates in the revised manuscript in section 2.1 as following:

"Before establishment of the park, some areas were used for low-intensity agriculture activities (Brockelman et al., 2011, 2017) that started at the end of 19th century or early twentieth century (Chanthorn et al., 2016)"

Reviewer #2, C4: *L.111: "SIS; n=3". This low number should be addressed in the discussion.*

Response C4: Please, see our response to Reviewer 1 comment C1.

Reviewer #2, C5 *L.114: If SES forest is 35-40 years old and OGS forest is more than 200 years old, what is in between?*

Response C5: Please see our response to *Reviewer #1 Comment 5.* Second-growth forests mostly have regenerated since the Park was established about 40-50 years ago. As a consequence, old (50-200 years) second-growth forests are very rare in the landscape so that the understory re-initiation stage is absent from our study. To better explain this, we added the following sentence in the revised manuscript.

"The classification is based on the framework of Oliver and Larson (1996) who studied successional gradients in temperate forests. Although the original framework considered four successional stages, we did not find any area corresponding to the understory re-initiation stage in the study landscape. Most second-growth forests have regenerated since the Park was established about 40-50 years ago so that older second-growth forests, where understory re-initiation occurs, is very rare in this area. In our study, the SES stage is represented by forest of upto 35-40 years, while other SES area in the landscape may typically range upto 55 years (since 1962), as suggested by some hand drawn historic maps (Smitinand, 1968; Cumberlege & Cumberlege, 1964). On the other hand, OGS forest stands mostly correspond to forests with no obvious sign of human disturbance during the last 100 years (Brockelman, 2011)."

Reviewer #2, C6: *L.160: "(see below)". Replace by "see Table S1"?*

Response C6: We agree, "(see below)" is replaced by "see Table S1" in the revised manuscript.

Reviewer #2, C7*: L.199-200: address "pixels that remained non-forest" (see General comment number 1)*

Response C7: Please see our response to your C2 comment.

Reviewer #2, C8: *L.206-208: This part of the methodology should be explained in more details, or differently. I wasn't sure what you meant until I saw Figure 5.*

Response C8: We agree that the sentence was quite unclear and reformulated it as following in the revised manuscript:

"We thus assigned to each pixel the year of the last non-forest to forest shift, if any, and considered this year as the forest recovery starting time. The AGB predicted by the LiDAR AGB map in 2017 was then used to estimate how much AGB was stored between the forest recovery starting time and 2017 through a non-linear power model."

Reviewer #2, C9: *L.225: separate the pixels that stayed non forest and those that stayed forest.*

Response C9: Please see our response to your C2 comment.

Reviewer #2, C10: *L.228: Do we know why? Is this addressed somewhere?*

Response C10: All cultivated areas were abandoned for natural reforestation after the park establishment in 1962 and a US Army camp was maintained open until the end of the Vietnamese war in 1975 (Chanthorn et al., 2016). By 1990's most of the study areas were thus reforested except few patches such as a golf course that reforested after 2001 (Chanthorn et al., 2016). **Because this historical dynamic is not accounted for in our analyses, we removed this sentence from the revised manuscript**.

Reviewer #2, C11: *L.233: Why only eight? Mention Figure S4?*

Response C11: We only considered the eight available secondary plots for which forest recovery start felt during the study period. The remaining field plots belong to the old growth forest type and were forested during the whole study period (see also Figure S4 of original manuscript, now Figure S5 in revised manuscript). To be more explicit we slightly reformulate the sentence as followed:

"Using field AGB estimates at two different census dates from eight secondary forest plots that started regenerating during the study period (see Figure S5) ,we showed that the observed rate of AGB accumulation was similar to the one predicted by our model and also tended to increase with forest age (in blue dots in Fig. 5)"

Reviewer #2, C12: *L.270-271: If the rate of accumulation is increasing, shouldn't the rate over 40 years be higher than the one over 20 years?*

Response C12: Thank you for identifying this counter-intuitive result. To produce those estimates, we used the formula of the model presented in Fig. 5 dividing the AGB predicted after 20 and 40 years by 20 and 40 respectively. If this approach would have been correct with no intercept in the model, you are right that it led to a counter-intuitive result with the existence of an intercept in the model. **Because the model should have an intercept to accurately capture the AGB dynamics, we now only report the rate of C accumulation during the first 20 years of succession to avoid ambiguity**. We revised the line as following in section 4.2:

"AGB accumulation in our study corresponds to a net carbon uptake of 3.4 Mg C ha−1yr−1 for the first 20 years."

Reviewer #2, C13: *Figure 1: add "(TCH)" in caption Figure 4: add grey classes to legend. Suggestion: Make distinction between "pixels that remained forest" and "pixels that remained nonforest"*

Response C13: Done, thank you.

Supporting information:

Reviewer #2, C14: *Table S1: Highlight the results of TCH and mention in caption that it is the best metric.*

Response C14: Done.

Reviewer #2, C15: *Table S2: Keep same name conventions as in TableS1. Are these the best 4 models?*

Response C15: We changed the names in Table S2 with the same name as given in Table S1. We tested TCH with additional metrics but adding a second predictor did not reduce the relative LOOCV-RMSE by more than 1% (mentioned in L171 in the original version of manuscript), so only TCH was selected as final predictor to avoid overfitting issues.

Reviewer #2, C16: *Figure S1: It would be nice to add the sub classes I mentioned about Figure 4, if possible.*

Response C16: Subclasses from Fig. 4 derived from the time series illustrated in Fig. S1 (now Fig. S2 in revised manuscript). At a given year, the only information that we can report for a pixel is its forest or non-forest status so that we cannot report the sub classes in the new Fig. S2.

Reviewer #2, C17: *Figure S2: Compare the histogram presented in Figure 3 to this one. Also, it would be nice to have some results from the random forest analysis somewhere in the Supporting Information and add that reference in the main text.*

Response C17: As recommended, we modified said Figure S2 (now Figure S3 in revised manuscript) by superimposing the density distribution from Figure 3. We also added the results of Random Forest showing the average variable importance in each Landsat sensor in Figure S1 in the revised manuscript. Both the revised Figure and new added Figure S1 is given:

Revised Figure S2 (Now Figure S3 in revised manuscript)

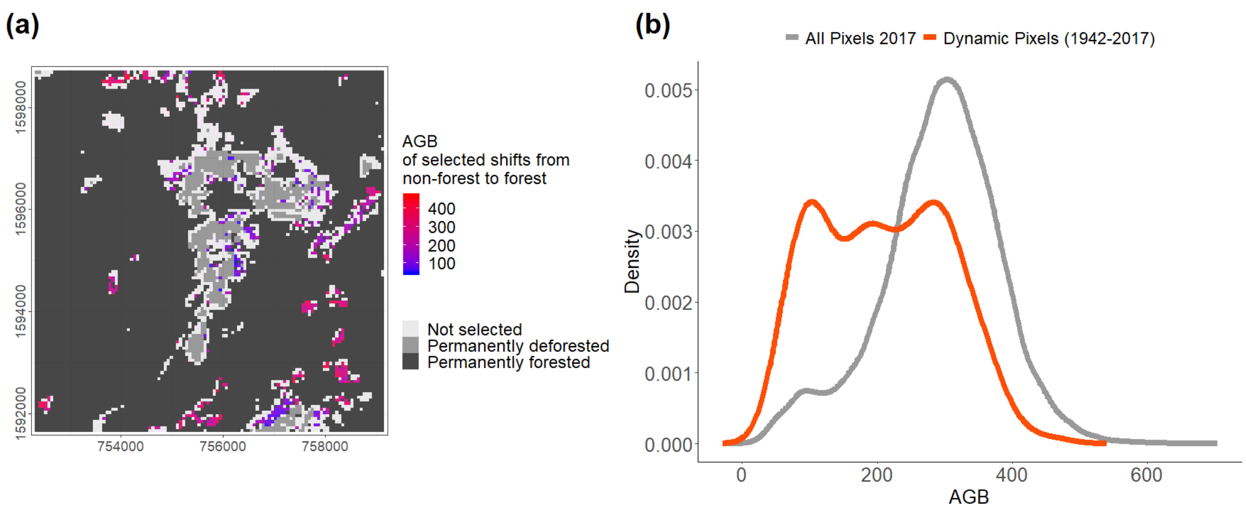

Addition of Figure S1: Random Forest analysis result

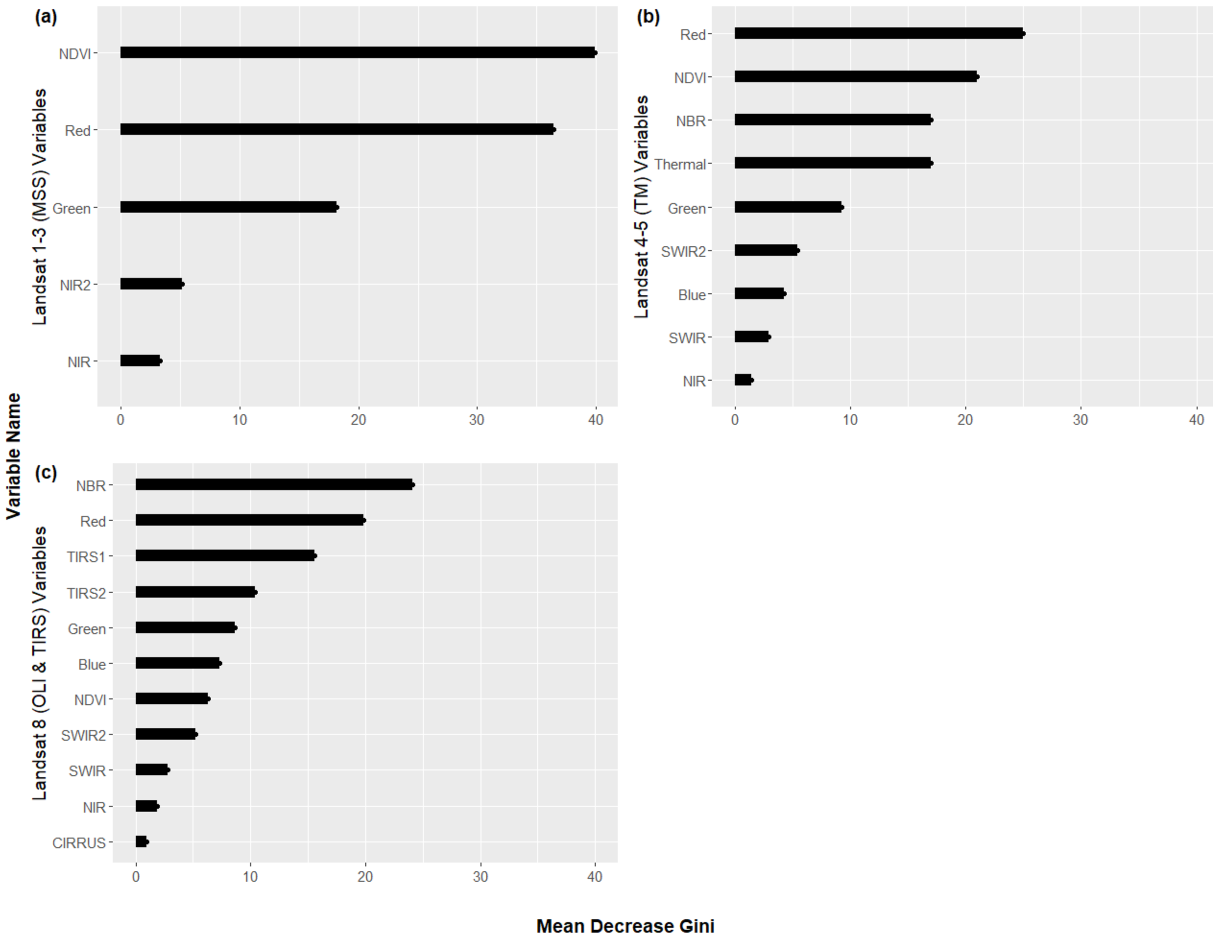

Minor comments:

Reviewer #2, C18: *L.36: Replace "The previous study" by "A recent study"*

Response C18: Done.

Reviewer #2, C19: *L.98: "which the plot officially joined": please rephrase*

Response C19: We rephrased the sentence as followed:

"Center for Tropical Forest Science (CTFS) network with which the plot is officially associated since 2009"

Reviewer #2, C20: *L.122: Replace "into the ground" by "into ground"*

Response C20: Done.

Reviewer #2, C21: *L.138: Replace "cannot" by "could not"*

Response C21: Done

Reviewer #2, C22: *L.211: For consistency, keep the order you present forest classes the same throughout the paper (SIS, SES, OGS)*

Reviewer #2, C22: We have now maintained the consistency of the forest classes as SIS, SES and OGS throughout the revised manuscript.

Response to the comments by Dr. Rico Fischer on "Forest aboveground biomass stock and resilience in a tropical landscape of Thailand"

Dear Dr. Fischer,

Thank you very much for the attentive assessment of our manuscript. We really appreciated your positive and constructive comments. Please find below our point-by-point responses to your *italicized* comments.

On behalf of the authors,

Nidhi Jha

Rico Fischer (RF): In this study, field data is combined with lidar data to estimate the biomass of secondary forest for a landscape in Thailand. In addition, Landsat scenes were used to distinguish forest and non-forest for the years 1972 to 2017. This made it possible to investigate the biomass dynamic of secondary forest in more detail. The study is very clearly structured and well written. The methodsTro are applied straightforward. This study is very interesting and very important, even if it was only studied for a small region in Thailand.

Response: Thank you

RF C1: *However, it is not clear to me why the authors did not used existing products and created their own products instead. A new biomass model is calibrated for the region in Thailand (from ALS with TCH as metric) – although there are already many studies on biomass estimation from ALS available with generalized models. Why calibrating a very specific equation for a small region? The same for the forest/non-forest maps. There are already products available (e.g. from Hansen or Sexton). Why generate your own product? There are certainly good reasons for this, but they should be discussed. In my view, the authors lose the opportunity to generalise this important study and apply them to larger regions.*

Response C1: RF is right that a few generalized LiDAR models were proposed in the literature (reviewed in Réjou-Méchain et al. 2019 Surveys in Goephysics). The most well-known generalized LiDAR model for tropical forests is from Asner et al. (2012, Oecologia), then updated in Asner & Mascaro (2014, Remote Sensing of Environment). If those generalized models may be useful with a limited availability of field data, they convey large systematic errors when transposed to new areas. For instance, they were reported to underestimate AGB by 7% (Jucker et al. 2017 *arXiv preprint*) and 16% (Réjou-Méchain et al. 2015 Remote Sensing of Environment) in two independent sites compared with locally adjusted models. When extensive field data is available locally, as in our case, there is no doubt that a locally-adjusted model is to be preferred, as recommended in Asner et al. (2012) and Asner & Mascaro (2014)'s papers.

A similar reasoning may be applied for the forest/non-forest maps products. While global products such as those proposed by Hansen and Sexton may be useful for some specific, large scale applications, they cannot outperform a locally-calibrated model that was trained with airborne LiDAR data. Even over large spatial scales, Landsat-based Global Forest Watch maps (Hansen) convey large systematic errors, e.g. a 24% underestimation of gross deforestation at the pantropical scale, with important continental variations (up to 92% in Humid tropical Africa, Tyukavina et al. 2015, Environmental Research Letters). Moreover, most global forest cover maps cover rather limited time periods, e.g. 2000- present for Hansen and 1990-present for Sexton, while we here consider a period of 42 years starting from 1975.

Further comments:

RF C2: *Title: The title is too general and does not address the specificity of the study – the forest carbon recovery in secondary forests for the last 42 years.*

Response C2: We still think that the title well reflects our study as we do also report forest carbon stock estimates. We let the editor decide if we have to change the title.

RF C3: *L 160: What are the lidar metrics? "see below" make no sense to me. Please refer to Table S1.*

Response C3: As suggested we have replaced "see below" by "see Table S1" in revised manuscript.

RF C4: *Equation 4: What is the spatial scale of the biomass estimation (AGB_L)? Is it 0.5ha? Please add the scale and also the r2 beside RMSE.*

Response C4: As suggested we have now added the spatial scale (0.5-ha) and the R^2 value (0.85) in section 3.1 of the revised manuscript as following:

"Among all the LiDAR metrics, the mean of top-of-canopy height (TCH, defined as the maximum height of 1-m resolution pixels) was the best predictor of field AGB estimates with a relative RMSE of 14% (RMSE = 45 Mg ha^{-1}; R^2= 0.85) at 0.5-ha scale"

RF C5: *Fig.2: The abbreviations (SIS, SES, OGS) only become clear if you read the whole text. It would be helpful to briefly explain the abbreviations here as well.*

Response C5: We agree. The full form of SIS, SES and OGS abbreviations are now provided in the caption of Figure 2.

RF C6: *Fig.3: Assuming Eq. 4 gives the biomass at the scale of 0.5ha, how can you generate with this a biomass map with the spatial scale of 60m?*

Response C6: We simply predicted AGB from a TCH estimated at 60-m resolution instead of 70-m resolution. The reason is that we had to calibrate the model with 0.5-ha field data and to produce a map matching the landsat resolution at 60-m resolution. We agree that this is not an ideal situation but, given that resolution remains very close and given that TCH is a mean, we do not believe that this impacted our results.

RF C7: *Fig.4: Why is there no transition from forest to non-forest? Could forest loss play a role in the results of the study?*

Response C7: There were only 70 pixels (0.5%) which shows single transition from forest to non-forest (Figure below). These pixels represent areas close to human-impacted areas (e.g., roads and national park tourism areas).

Since our study area is a protected zone, forest loss is very limited and hence does not play an important role in the overall dynamics.

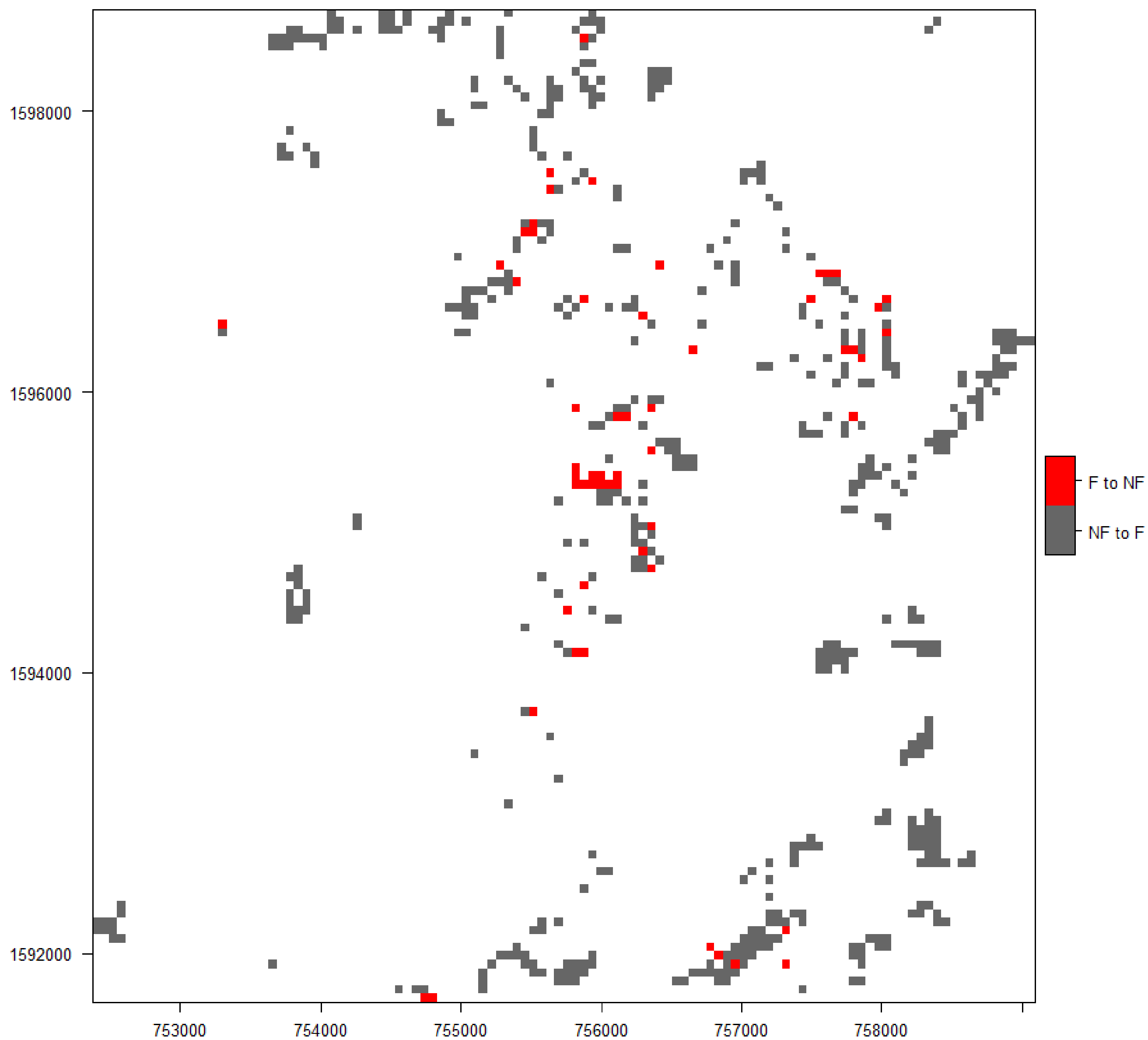

Figure: Pixels in red shows the pixels that underwent Forest to Non-forest shifts (F to NF) with the other selected pixels that has underwent Non-Forest to Forest (NF to F)

RF C8: *Fig.5: This figure shows that the secondary forest allocates more and more biomass as it becomes older. But if you look at Fig. 3, you can see the highest biomass values between 300 and 400 Mg/ha. Shouldn't Fig.5 therefore show saturation in the AGB recovery at some point? Possibly a power model (red line) is not suitable as a model due to the unlimited growth, but rather a model with a capacity limit*

Response C8: As discussed in the manuscript, we agree that a saturation should rapidly occur, typically after 50 years. This is the reason why we assume, as previous authors did, that the overall functional form should rather be a sigmoid form. However, our time period stopped at 42 years so that a power model was more adapted to our data. We however agree that this model cannot be used outside the calibration model domain, i.e. for forests older than 42 years.

Forest aboveground biomass stock and resilience in a tropical landscape of Thailand

Nidhi Jha[1~~,2~~], Nitin Kumar Tripathi[1], Wirong Chanthorn[2~~3~~], Warren Brockelman[3~~4~~], Anuttara Nathalang [3,4~~,5~~], Raphaël Pélissier[5~~2~~], Siriruk Pimmasarn[1], Pierre Ploton[5~~2~~], Nophea Sasaki[6], Salvatore G.P. Virdis[1], Maxime Réjou-Méchain[5~~2~~]

1~~Field of Remote Sensing and GIS (RSGIS),~~ Department of Information & Communication Technologies, School of Engineering and Technology (SET), Asian Institute of Technology, Thailand.

~~[2]AMAP IRD, CNRS, CIRAD, INRA, Univ Montpellier, Montpellier, France.~~

[2~~3~~]Faculty of Environment, Kasetsart University, Thailand

[3~~4~~]National Center for Genetic Engineering and Biotechnology (BIOTEC), Thailand

[4~~5~~]National Biobank of Thailand (NBT), Pathum Thani, Thailand

[5]AMAP IRD, CNRS, CIRAD, INRA, Univ Montpellier, Montpellier, France.

[6]Department of Development and Sustainability, Asian Institute of Technology, Thailand

Correspondence to Nidhi Jha (nidhi23aug@gmail.com)

Abstract. Half of Asian tropical forests were disturbed in the last century resulting in the dominance of secondary forests in Southeast Asia. However, the rate at which biomass accumulates during the recovery process in these forests is poorly understood. We studied a forest landscape located in Khao Yai National Park (Thailand) that experienced strong disturbances in the last century due to clearance by swidden farmers. Combining recent field and airborne laser scanning (ALS) data, we first built a high-resolution aboveground biomass (AGB) map over 60 km^2 of the forest landscape. We then used the random forest algorithm and Landsat time-series (LTS) data to classify landscape patches as non-forested versus forested on an almost annual basis from 1972 to 2017. The resulting chronosequence was then used in combination with the AGB map to estimate forest carbon recovery rates in secondary forest patches during the first 42 years of succession. The ALS-AGB model predicted AGB with an error of 14% at 0.5-ha resolution (RMSE = 45 Mg ha^{-1}) using the mean top-of-canopy height as a single predictor. The mean AGB over the landscape was of 291 Mg ha^{-1} showing a high level of carbon storage despite past disturbance history. We found that AGB recovery varies non-linearly in the first 42 years of the succession, with an increasing rate of accumulation through time. We predicted a mean AGB recovery rate of 6.9 Mg ha^{-1} yr^{-1}, with a mean AGB gain of 143 and 273 Mg ha^{-1} after 20 and 40 years, respectively. This rate estimate is about 50% larger than the new prescribed IPCC 2019 rate for young secondary asian tropical rainforests but close to the previous IPCC 2006 rates. Our recovery estimates are also within the range of those reported for the well-studied Latin American secondary forests under similar climatic conditions. This study illustrates the potential of ALS data not only for scaling up field AGB measurements but also for predicting AGB recovery dynamics when combined with long-term satellite data. It also illustrates that tropical forest landscapes that

were disturbed in the past are of utmost importance for the regional carbon budget and thus for implementing international programs such as REDD+.

1 Introduction

Tropical forest disturbances and subsequent biomass recovery through time significantly affect the global carbon cycle (Harris et al., 2012). Although secondary forests in the tropics could constitute a major global carbon sink, the magnitude of such sink remains poorly known (Chazdon, 2014; Lugo and Brown, 1992). A previous study estimated that 40 years of carbon storage in regenerating tropical forests from Latin America offset the past 19 years of carbon emissions from fossil fuels and industrial production at the scale of Latin America (Chazdon et al., 2016).~~The previous study has found that this carbon sink is accountable for absorbing half of the carbon emissions from fossil fuels and industrial production at the scale of Latin America (Chazdon et al., 2016).~~ Thus, there has been much interest in quantifying the ability of tropical secondary forests to sequester carbon in order to reduce uncertainties in the global carbon balance (e.g., Chai, 1997; Lohbeck, Poorter, Martínez-Ramos, & Bongers, 2015; Stas, et al., 2017).

Previous studies have used long-term forest plot surveys along chronosequences to quantify forest carbon dynamics in secondary tropical forests (Chazdon et al., 2007; N'Guessan et al., 2019; Norden et al., 2011, 2015; Poorter et al., 2016a; Rozendaal and Chazdon, 2015). Although long-term forest plots are essential for understanding the dynamics of tropical forests (Losos and Leigh, 2004), they are scarce, inherently labor-intensive, expensive and time-consuming to maintain, and not evenly distributed in the tropics. In addition, most studies of carbon dynamics along tropical forest successions are concentrated in Latin America (Chave et al., in press) ; Letcher and Chazdon, 2009; Norden et al., 2015; Poorter et al., 2016a; Rozendaal et al., 2017; Rozendaal and Chazdon, 2015 but see N'Guessan et al., 2019 in Africa). They show high among-site variation in forest carbon recovery rates, suggesting a high context-dependence (Chazdon et al., 2007; Norden et al., 2011, 2015), partly depending on climate conditions (Poorter et al., 2016a). A few pantropical studies have shown that the carbon potential of Latin American forests is smaller than that of Southeast Asian and African forests (Feldpausch et al., 2012; Sullivan et al., 2017). However, a recent review study based on limited data from Asia surprisingly estimated that the forest carbon sequestration potential of tropical secondary rainforest in Asia is much lower than in the American and African rainforests, leading to updated IPCC recommendations (Requena Suarez et al. 2019). Whether these new estimates are representative of Asian tropical rainforests is highly uncertain, due to a lack of data. This issue is especially crucial for Asian tropical forests where half of the forests have been disturbed during the last century, resulting in the dominance of secondary forests throughout the region (Achard et al., 2014; Mitchard et al., 2013; Stibig et al., 2014).

Remote sensing technology has emerged as a promising tool for extrapolating local field carbon estimates over landscapes, regions, or at the global scale (Gibbs et al., 2007; Goetz et al., 2009). However, current long-term (>20 years) satellite data such as Landsat are weakly sensitive to forest carbon, especially in high-biomass forests (Ferraz et al., 2018; Lu, 2006; Meyer et al., 2019; Zheng et al., 2004). Yet, these data may be used to produce reliable land-cover classifications (e.g., forest versus non-forest areas; FAO 2010). They allow to assess the dynamics of deforestation and reforestation worldwide (Hansen et al., 2013) and can thus monitor disturbance history, particularly the time since abandonment of agriculture (Cohen et al., 1996; Masek and

Collatz, 2006). However, the forest carbon dynamics associated with such deforestation and reforestation events remains highly uncertain due to the large uncertainties of global carbon maps (Mitchard et al., 2013, 2014; Réjou-Méchain et al., 2019).

On another hand, airborne laser scanning (ALS) provides accurate landscape-scale estimates of forest structural parameters (Maltamo et al., 2005; Næsset, 2002; Wulder et al., 2012). When calibrated with field-based estimates of aboveground biomass (AGB), ALS metrics can be used to produce high-resolution forest carbon maps, even for high carbon-dense tropical forests (Asner et al., 2010; Cao et al., 2016; Ferraz et al., 2018; Kronseder et al., 2012; Labriere et al., 2018; Zhao et al., 2009; Zolkos et al., 2013). Multi-temporal ALS acquisitions may thus provide direct estimates of the carbon balance of tropical forest landscapes (Dubayah et al., 2010; Meyer et al., 2013; Réjou-Méchain et al., 2015). However, due to its relatively recent emergence, ALS technology cannot be used to investigate long-term dynamics directly yet (>10 years).

Combining long-term (>40 years) land cover change assessment from satellite data archives (e.g., Landsat) and contemporary LiDAR AGB maps may be a promising avenue for understanding the long-term forest carbon dynamics. Such an approach has been successfully implemented in temperate and boreal forests (Bolton et al., 2015; Pflugmacher et al., 2012, 2014; White et al., 2018; Zald et al., 2014). However, to our knowledge, it has not been yet used to assess the forest carbon resilience of tropical forests (but see Helmer et al., 2009 who used satellite-based LiDAR).

In this study, we combined extensive field, ALS, and LTS data to assess the spatial variation of AGB and forest AGB dynamics of secondary forests in a Thai landscape. More specifically, we first calibrated a robust ALS-AGB model to produce a fine-scale AGB map at the landscape scale. We then used a random forest machine-learning algorithm to classify historical Landsat images from 1972 to 2017 into forest and non-forest classes. Using this information over time, we generated a cumulative forest gain map over a period of 42 years of succession. We finally combined this chronosequence with our ALS-AGB map to estimate the forest carbon resilience of secondary forests during the 42 first years after land abandonment.

2. Materials and methods

2.1 Study area

The study area of ca. 6,400 ha is part of Khao Yai National Park in central Thailand (latitude: 14° 25' 20.4" N, longitude: 101° 22' 36.9" E; Fig. 1). Khao Yai is the first national park of Thailand, established in 1962. It is home to numerous endangered plant and animal species (Kitamura et al., 2004). The area receives approximately 2,200 mm of precipitation annually, with a dry season of five to six months (precipitation below 100 mm month^{-1}) from November to April (Brockelman et al., 2011; Chanthorn et al., 2016). The annual mean temperature is about 22–23°C (Jenks et al. 2011), and the altitude of the study area varies from 650 m to 870 m. Before establishment of the park, some areas were used for low-intensity agriculture activities (Brockelman et al., 2011, 2017) that started at the end of 19th century or early twentieth century (Chanthorn et al., 2016) and then naturally reforested at different times depending on when burning ceased (Chanthorn et al., 2016). As a consequence, the landscape constitutes a mosaic of secondary forests of different ages amidst old-growth forests (Chanthorn et al., 2016).

2.2 Field data

We used three sets of forest inventory plots with a total sample area of 35 ha (Fig. 1). First, a large 30-ha contiguous (500 m × 600 m) forest dynamics plot, named Mo Singto, was established in old-growth forest after 1998 and completely censused in 2004–2005, 2010–2011 and 2016–2017. The census method follows the protocol of the Center for Tropical Forest Science (CTFS) network with which the ~~the~~ plot is officially ~~joined~~ associated since~~in~~ 2009 (Brockelman et al., 2011). The second set of plots included eight separate 0.48-ha plots (60 m × 80 m) that were established from March to May 2013 and re-censused from November 2017 to January 2018 (Chanthorn et al., 2017). These plots are set along a successional gradient varying from near stand initiation to old-growth forest. Lastly, a 1-ha plot (100 m × 100 m) located near the north border of the 30-ha Mo Singto plot was established in a secondary forest in 2005 and then re-censused in 2010 and 2017. In all plots, trees ≥1 cm in diameter at breast height (dbh) were tagged, identified to species, mapped and measured for their diameter, except in the 0.48-ha plots where the minimum dbh was 4 cm. A total of 184,239 individual trees were measured across all the plots, from which 517 trees were measured for height using a pole for short trees (<5 m), a laser range finder (Nikon Forestry 550) for medium height trees (5–7m) and a Vertex III hypsometer for tall (>7 m) trees (Chanthorn et al., 2017). In this paper, we used the 2017 census data, concomitant with the ALS campaign, to estimate AGB and multiple censuses to estimate the AGB dynamics of secondary plots. For the sake of homogeneity in tree measurements, we used only trees ≥5 cm in dbh in the whole dataset.

In order to homogenize plot size, we subdivided all plots ≥1 ha into 0.5-ha subplots. This resulted in 70 plots of either 50 m × 100 m (n = 62) or 60 m × 80 m (n = 8) that we classified in three successional stages from young to old-growth forests following the classification from (Chanthorn et al., 2017): Stand initiation (early) stage (SIS; n = 3); stem exclusion (intermediate) stage (SES; n = 5), and old growth stage (OGS; n = 62). This classification followed the framework of Oliver and Larson (1996) who studied successional gradients in temperate forests. Although the original framework considered four successional stages, we did not find any area corresponding to the understory re-initiation stage in the study landscape. Most second-growth forests have regenerated since the Park was established about 50 years ago so that older second-growth forests, where understory re-initiation occurs, is very rare in this area. Based on interviews of senior park rangers and using Landsat remote sensing data, Chanthorn et al., (2017) estimated that the age of the forests was approximately 15–20 years for SIS forests, 35–40 years for SES forests and unknown but probably older than 200 years for OGS forests. Note that the SES stage is represented by forest of upto 35-40 years in our study but other SES area in the landscape may typically range upto 55 years (since 1962), as suggested by some hand drawn historic maps (Cumberlege & Cumberlege, 1963; Smitinand, 1968). On the other hand, OGS forest stands mostly correspond to forests with no obvious sign of human disturbance during the last 100 years (Brockelman, 2011).

2.3 ALS data

The airborne laser scanning (ALS) campaign was conducted on 10 April 2017 over ca. 64 km^2 (Fig. 1). The Asian Aerospace Services Limited company (Bangkok) acquired the ALS data with a RIEGL LMS Q680i installed into a Diamond Aircraft "Airborne Sensors" DA-42 fixed-wing plane. The flying altitude was about 500–600 m above ground level with a 60-degree field of view, and a pulse repetition frequency of 400 kHz, for which the aircraft maintained an average ground speed of 185 km hr^{-1} capturing the area of interest in 50 overlapping laser strips. We discretized the full waveform data for subsequent analyses resulting in an average point density of ca. 22 points m^{-2}.

Post-processing of ALS data and point cloud classification into ~~the~~ ground, vegetation, or noise were done using TerraScan of Terrasolid Version 14. Points classified as ground were used to build a digital terrain model (DTM) at 1-m resolution using a k-nearest neighbour kriging approach implemented in the LidR R package (Roussel and Auty, 2017). A 1-m resolution canopy height model (CHM) was then computed from the height of the normalized vegetation points, discarding outliers classified as air or noise. Finally, we used the CHM and the normalized vegetation point cloud to derive different forest height metrics ~~(L-metrics)~~ at the plot level (Table S1).

2.4 Landsat data

We retrieved Landsat images (MSS, TM, OLI and TIRS products) for the study area from the Landsat archive (**http://glovis.usgs.gov**) between the 1972–2017 period (WRS-1 138/50 and WRS-2 path/row: 129/50). To minimize the impact of clouds and potentially varying phenology within years, we mostly selected images acquired during the dry season, from November to March. We thus collected Landsat 1-3 MSS data (1972–1983), Landsat 4-5 TM (1984–2011), and Landsat 8 OLI & TIRS (2013–2017) data. We did not consider Landsat 7 ETM+ images due to the failure of the Scan Line Corrector, leading to data gaps. All Landsat images were already orthorectified and displayed an accurate co-registration with ALS data. Before 1984, Landsat MSS collected data at 60 m × 60 m spatial resolution in most bands. Thus, to have consistent time series data, we aligned all the post-1983 Landsat data using a reference image from 1972 and aggregated each image to 60 × 60 m. Over the 44 years, we selected a total of 34 high-quality images, each representing one year. For the 11 missing years, we could not find cloud-free images and no image was available in 2012 since we discarded Landsat 7 ETM+ data.

2.5 Field aboveground biomass calculation

We estimated tree aboveground biomass (AGB) using a pantropical allometric model (Eq. 4 from Chave et al., 2014). This model uses the diameter (D), total tree height (H) and wood density (WD) as the predictors and was shown to hold across tropical vegetation types and regions. Wood density was estimated using species (47% of stems), genus (50%) or stand (3%) averaged values from the global wood density database (Chave et al., 2009; Zanne et al., 2009). Tree height was estimated through locally-adjusted height-diameter (H-D) models of the form given in Eq. (1):

$$ln(H) = a + b \times ln(D) + c \times ln(D)^2 + \varepsilon \quad (1)$$

where a and b are model parameters to be adjusted and ε is a normally distributed error with mean 0 and standard error $\sigma logH$. Tree height was subsequently estimated using the back-transformation formula including a known bias correction (Baskerville, 1972) using following Eq. (2):

$$H = exp\left(0.5 \times \sigma_{logH}^2 + a + b \times ln(D) + c \times ln(D)^2 + \varepsilon\right) \quad (2)$$

Because H-D relationship varies along the successional gradient (Chanthorn et al., 2017), we fitted three independent H-D models for the three different successional growth forest stages using 177 measured trees for SIS plots, 159 for SES plots and 181 for OGS plots.

AGB at the plot level was then estimated in Mg ha^{-1} by summing individual tree AGB for all trees with dbh ≥ 5cm belonging to the plot. We did all these analyses using the R BIOMASS package (Réjou-Méchain et al., 2017).

2.6 LiDAR AGB model

We relied on a log-log model form given in Eq. (3) to model AGB from ALS data (Asner et al., 2012; Réjou-Méchain et al., 2015):

$$ln(AGB\ \ ) = a + b \times ln(L1) + c \times ln(L2) + \ldots + \varepsilon \qquad (3)$$

Where *L1*, *L2*, … are the LiDAR metrics to be selected (see Table S1)~~(see below)~~ and *ε* the error term assumed to be normally distributed with zero mean and residual standard error *σlogL*. Fitting the model with log-transformed variables allows us to model a multiplicative error and thus to account for higher model prediction error with larger AGB values (Zolkos et al., 2013). Using this model, we selected the most predictive LiDAR metrics from our full set of LiDAR metrics using a leave-one-out-cross-validation (LOOCV) scheme nested within a forward selection procedure. The LOOCV consists of fitting models with all observations except one, and then using the model to predict the value of the observation held out of model calibration. The process is repeated for all observations so that model prediction accuracy, here the root mean squared error (RMSE), can be independently assessed from all observations. This LOOCV approach was repeated for different models following a forward procedure that begins by selecting the most discriminant variable according to the LOOCV-RMSE criterion. The procedure then continues by selecting the second most discriminant variable and so on. To minimize the problem of model overfitting, we only kept explanatory variables that contribute to a decrease in relative RMSE (RMSE divided by the mean observed AGB) by more than 1%. The selected LiDAR-AGB model was then used to predict AGB values over the Landscape at 60-m resolution, to match the resolution of Landsat images.

2.7 AGB recovery analysis

2.7.1 Forest-non-forest classification

To classify areas as forest or non-forest, we applied the random forest (RF) algorithm independently on each Landsat image to minimize inter-images classification error that may otherwise arise from instrumental (e.g. differences in sensors spectral characteristics) and phenological effects. We used all Landsat bands and their ratios as predictors in our RF classification models i.e. the 4 raw bands for Landsat 1-3 MSS data (1972-1983), the 7 raw bands for Landsat 4-5 TM (1984-2011) and the 9 raw bands for Landsat 8 OLI & TIRS (2013-2017). The normalized difference vegetation index (NDVI) was additionally used as a predictor for all the sensors while the normalized burn ratio (NBR) was only used for Landsat 4-5 and Landsat 8 due to non-availability of SWIR bands in MSS sensors. Thus, we used 18 predictors for MSS, 51 predictors for TM and 83 for OLI & TIRS as an input for the RF algorithm. RF model for each year of the study period was then trained on the same set of pixels that likely remained either forested or non-forested from 1972 up until 2017. This training dataset was built using the 2017 ALS data. We first aggregated the 1-m LiDAR-derived CHM at the same resolution as the Landsat images (60-m resolution) and defined non-forest pixels as pixels having a mean top of canopy height < 5 m (FAO, 2012; Sasaki & Putz, 2009). Because 60-m scale deforestation is unlikely to have occurred in the area since the establishment of the national park in 1962, areas that were classified as non-forest with the 2017 LiDAR data very likely corresponded to non-forested areas during the whole study period. By contrast, we defined as forested areas all 60-m pixels that had a LiDAR mean top of canopy height > 30 m because these tall forests very likely corresponded to forested areas during the whole study period. We thus used a reference set of 400 60-m pixels classified as non-forest and 110 as forest. This dataset was then randomly divided into a training dataset (60%) to calibrate the RF models and a validation dataset (40%) to assess the accuracy of the forest and non-forest classification. We only considered classified pixels that had a post-probability of assignment >90% in the RF outputs (Pickell et al., 2016; White et al., 2018) and calculated the classification accuracy as the proportion of pixels that were correctly classified as forest or non-forest in the validation dataset. This statistical analysis was done using the "randomForest" R package (Liaw and Wiener, 2002).

2.7.2 Forest AGB recovery analysis

We combined time-series classified Landsat images with the 60-m resolution LiDAR AGB map to quantify AGB recovery as a function of time. We used classified time-series data to assign to each pixel the last date at which a shift from a non-forest to forest status occurred during the study period. Thus, all pixels that did not experience any shift, i.e. that remained non-forested or forested during the whole study period were discarded from this analysis. To minimize false detection of land cover change due, for example, to atmospheric pollution, we only considered shifts that entailed land cover change for at least two consecutive images. Thus, we did not consider any shift before 1975 because, to be considered, the non-forest to forest shift of a pixel should occur after being classified as non-forest in the two previous images (in our case in 1972 and 1973). Finally, we also discarded pixels that underwent more than four different shifts during the whole study period because numerous shifts are likely to indicate areas prone to forest degradation, e.g. close to human occupancy areas such as roads, introducing a bias in our inferences on the natural successional dynamics. We thus assigned to each pixel the year of the last non-forest to forest shift, if any, and considered this year as the forest recovery starting time. The AGB predicted by the LiDAR AGB map in 2017 was then used to estimate how much AGB was stored between the forest recovery starting time and 2017 through a non-linear power model.

3. Results

3.1 Forest biomass stocks

Field plots AGB ranged from 80 to 577 Mg ha^{-1} (mean of 315 Mg ha^{-1}), with a mean AGB of SIS, SES and OGS plots of 87 Mg ha^{-1}, 291 Mg ha^{-1} and 328 Mg ha^{-1}, respectively. Among all the LiDAR metrics, the mean of top-of-canopy height (TCH, defined as the maximum height of 1-m resolution pixels) was the best predictor of field AGB estimates with a relative RMSE of 14% (RMSE = 45 Mg ha^{-1}; R^2= 0.85) at 0.5-ha scale (Fig. 2). Adding a second predictor did not reduce the relative RMSE by more than 1% (Table S2). We thus kept TCH as a single predictor for our analyses resulting in the following Eq. (4) for LiDAR-AGB model:

$$AGB_L = 4.30 \times TCH^{1.39} \qquad (4)$$

Using this LiDAR-AGB model, we predicted AGB over the whole landscape (Fig. 3a). The distribution of AGB values over the landscape was not normally distributed due to an over-representation of pixels with low AGB values. At the landscape scale, predicted AGB ranged from 0 to 681 Mg ha^{-1} with a mean of 291 Mg ha^{-1} (Fig. 3b), close to the mean AGB of the field plots.

3.2 AGB recovery analysis

Our forest and non-forest classification through time was highly accurate, with 90% to 99% of well-classified validation pixels in individual classified images (Table S3, Fig. S1-2). Figure 4a illustrates the resulting spatialized time series of non-forest-to-forest shifts over the study area and showed that most (83%) of the landscape did not experience such shift at 60-m resolution, out of which 5% of the area remained permanently non-forested over the 42-year study period. Most of these non-forested areas were continuously cleared and mostly correspond to National Park buildings, including tourist shops and guest houses~~-~~ or camping location. Over the 17% remaining pixels that experienced a shift, we concentrated our analyses on the 4% pixels (n = 550; ca. 198 ha) that passed our selection procedure and that were well distributed over the landscape (Fig. 4a). ~~Of all these selected pixels almost 60% of the shifts occurred before 1990 (Fig. 4b)~~.

Considering the selected pixels that experienced a shift from non-forest to forest, we found that AGB accumulated non-linearly through time during the 42 first years of the succession (Fig. 5). A simple power model led to a pseudo-R^2 of 0.66 and a power exponent greater than 1, indicating an increase in the rate of AGB accumulation with recovery time. This model predicts an AGB gain of 143 Mg ha^{-1} after 20 years of recovery and of 273 Mg ha^{-1} after 40 years (spatialized gain in AGB is shown in Fig. S3). Using field AGB estimates at two different census dates from eight secondary forest plots that started regenerating during the study period (see Figure S5), we showed that the observed rate of AGB accumulation was similar to the one predicted by our model and also tended to increase with forest age (in blue dots in Fig. 5). Finally, focusing on the 17% pixels that experienced at least one shift from non-forest to forest since 1972, we estimated that the study area has stored a minimum AGB of 455 Gg, as observed in the 2017 LiDAR AGB map, equivalent to 214 GgC during the study period.

4. Discussion

In this study, we showed that the integration of field inventory, Landsat archives, and LiDAR data provide a powerful approach for characterizing the spatio-temporal dynamics of aboveground biomass in tropical forests. While the carbon stocks and recovery potential of south-Asian tropical forests are globally poorly known, our approach contributes to a better understanding of the role of these forests in global carbon dynamics. We specifically showed that our study site stores a large amount of carbon, despite its disturbance history, and ~~probably~~ acts as a strong carbon sink, through secondary succession pathways.

4.1 Spatial variation in AGB

Using extensive field data, we have shown that forest AGB can be predicted with an error of 14% at a 0.5-ha resolution using a single LiDAR metric, the mean top-of-canopy-height (TCH), a metric previously identified as a robust predictor of AGB (Asner and Mascaro, 2014). This error typically falls within the range of expected errors at this resolution (Zolkos et al., 2013). Using a robust metric selection approach, we showed that adding any other LiDAR metrics did not bring any additional information and that our single predictor did not show any saturation for large AGB values. Many studies have used a combination of several LiDAR metrics selected through less robust approaches, i.e. not through independent validation approaches such as our LOOCV procedure, potentially generating overfitting problems (Junttila et al., 2015). We here confirm, similarly to Asner et al. (2012) and Réjou-Méchain et al. (2015), that simple parsimonious models should be preferred, at least within a given tropical forest landscape. Due to a limited number of field plots in low-biomass areas we were, however, unable to test whether predicting errors vary with AGB or not.

Using this LiDAR model, we predicted a mean AGB over the landscape of 291 Mg ha^{-1}, corresponding to a carbon density of 137 MgC ha^{-1} (using a ratio of biomass to carbon conversion of 0.47; Thomas and Martin, 2012). Using a large network of field plots, a recent pantropical study suggested that Southeast Asian and African forests store significantly more carbon than Amazonian forests (Sullivan et al., 2017). However, in this latter study, Southeast Asian forests were only represented by field data from Indonesia and Malaysia where trees are known to be particularly tall (Coomes et al., 2017; Feldpausch et al., 2011; Jucker et al., 2017, 2018). Here, we found that our study forests stored significantly less carbon than forests in Indonesia and Malaysia, where the mean carbon density reached ca. 200 MgC ha^{-1} (Sullivan et al., 2017), but as much as in Amazonian forests (mean of 140 MgC ha^{-1}; Sullivan et al., 2017), even when considering only old-growth forest plots. Whether the relatively low carbon density of our study site, compared to other Southeast Asian forests, is specific to our study area or representative of other Southeast Asian forests should be further investigated.

We found a very high spatial heterogeneity of AGB at the landscape scale with an apparent over-representation of low AGB values. This is most probably the consequence of past human activities in this area up to the establishment of the park that led to the present mosaic of secondary and mature forests. This result indicates that this area is currently likely to be a net carbon sink.

4.2 AGB recovery through time

Combining classified images obtained from LTS and LiDAR data, we quantified the recovery rate of forests after land abandonment. As expected, we showed a significant increase of AGB with recovery time. After 20 years of recovery, our model predicts an AGB accumulation of 143 Mg ha^{-1}, an estimate slightly higher than the one predicted by Poorter et al., (2016a) in Neotropical secondary forests (122 Mg ha^{-1}). However, this difference can partly be explained by the inclusion of trees between 5 and 10 cm dbh in our study, contrary to Poorter et al., (2016)'s study. AGB accumulation in our study corresponds to a net carbon uptake of 3.4 Mg C $ha^{-1}yr^{-1}$ for the first 20 years. This rate of carbon accumulation over the first 20 years of succession is close to the pantropical estimate from Silver et al., (2000) and is also similar to the previous default continent recovery rates given by IPCC guidelines (IPCC, 2006). However, the recent refinement of IPCC default rates halved this estimate for young asian secondary rainforest (≤ 20 years) (Requena Suarez et al. 2019), suggesting that young secondary forests store carbon at a much lower rate in Asia than in Latin America or in Africa. This new estimate derived from very limited data (7 chronosequences), not necessarily representative of asian tropical rainforests, and including very small field plot data (≤ 10 m in size; Hiratsuka, et al., 2006; Ewel et al., 1983), potentially resulting in important sampling errors (Réjou-Méchain et al. 2014). Given the huge implications of these updated IPCC default rates for Asian countries, we here call for testing in other areas whether these new IPCC rates strongly underestimate the carbon potential of forest regrowth in tropical Asia, as found in this study.

Our model showed that a non-linear power model with an exponent > 1 best fit our data, suggesting an increase in the rate of carbon accumulation during the first 42 years of succession.

Contrary to the results found by Feldpausch et al. (2007), the rates of AGB accumulation inferred with our approach provided estimates similar to those obtained from long-term field plot surveys (Fig. 5), validating the chronosequence approach in our study area. Assuming that the carbon recovery rate rapidly decreases after 50–60 years (Brown and Lugo, 1990; Silver et al., 2000), our result suggests a sigmoid relationship of AGB accumulation with time in our study area. Previous studies have shown different models of AGB accumulation with forest age. Saldarriaga et al. (1988) showed that the AGB of Neotropical forests from the upper Rio Negro increased linearly with stand age during the 40 years, while Jepsen, (2006) reported a sigmoidal increase in AGB accumulation in Sarawak, Malaysia, as is likely the case in our study area. Finally, working on 41 Neotropical sites, Poorter et al. (2016a) assumed a logarithmic trend in the AGB accumulation over time, hence a decrease of the rate of carbon accumulation through time, probably because they investigated a longer time period. Selecting the sites of Poorter et al. (2016a, 2016b) that had at least 10 observations over the first 44 years (n = 21 out of 28 sites, i.e. excluding 7 sites for which model fitting was not possible), site-specific power models revealed that two-thirds of the sites displayed a power exponent <1 and one-third showed an exponent >1 (Fig. S4). Thus, the accumulation of AGB with age follows different trends across sites, as already highlighted in previous studies (Kennard et al., 2002; Poorter et al., 2016a; Ray and Brown, 2006; Ruiz et al., 2005; Silver et al., 2000; Toledo and Salick, 2006). Understanding how these trends vary according to abiotic factors (e.g. soil type, rainfall), species assemblage and diversity, or to priority effects such as types of land use and land management existing before forest recolonization, constitutes an important research perspective (Chazdon, 2014; McMahon et al., 2019).

Our analysis was based on a forest/non-forest classification through time and our independent validation suggested a high overall accuracy (90 to 99%), similar to that reported by other studies using Landsat data classification in boreal systems (Bolton et al., 2015; White et al., 2018). Furthermore, our estimate of forest age using this approach was highly consistent with our expectations. Indeed, using our forest plots, we found that the SES and SIS forest stages lasted on average 40 years (range 38–42) and 13 years (range 8–20), respectively, hence very close to suggestions of Chanthorn et al. (2017) (Fig. S5). However, our overall approach cannot be replicated easily in human-occupied areas. Indeed, human disturbances lead to forest degradation that, in contrast to deforestation, is not captured by the Landsat signal, so that, when combined with a reference AGB map, natural carbon recovery potential could be seriously underestimated. Because our study area was protected from human disturbances during the study period, we were in very favourable conditions to estimate forest carbon recovery rates and strongly encourage researchers benefiting from similar conditions to replicate our analyses in other study sites.

5 Conclusions

Our study demonstrates that combining field, LiDAR, and long-term satellite data provides an efficient way to assess forest carbon recovery rates during secondary successions. We showed that it produces similar estimates as those inferred from long term field plots, but at a much lower cost and within a much shorter time frame. Replicating this approach in other protected tropical landscapes, notably in the Asian subcontinent, would thus considerably increase the representativeness of forest carbon recovery rates. This would probably improve our understanding of the environmental and historical drivers of these varying rates between ecological zones and continents. This is especially important in Southeast Asian forests that constitute a hotspot of biodiversity and carbon, and that are under threat due to the fast changing of both environment and socio-economics in this region. Quantifying the rates at which different forest types accumulate carbon should thus stay at the forefront of the research agenda and would greatly benefit the Earth system model community and international policy initiatives such as REDD+.

Code availability/Data availability

Code and data are available upon request to the corresponding author.

Author contribution

NJ, NKT, and M~~N~~RM designed the study; NJ and M~~N~~RM analyzed the data and wrote the first draft of the paper; WC, WB, and AN provided field data. All authors provided valuable feedbacks on analyses and the manuscript.

Competing interests

The authors declare no competing interest.

Acknowledgments

This study was supported by the project (AIT/SET - 2016 - R011) sponsored by the French Ministry of Foreign Affairs, and International Development initiated during the Regional Forum on Climate Change. We gratefully thank the National Science and Technology Development Agency (Thailand) for supporting the long-term monitoring of all forest plots and the Department of National Parks, Wildlife and Plant Conservation (DNP) that supported our research. NJ benefitted from an Eiffel excellence scholarship French program and a mobility grant from the IRD institute for long stays (9 months) in the AMAP labarotary. RP, PP and MRM were supported by the project 3DForMod funded by ERA-GAS (ANR-17-EGAS-0002-01).

References

Achard, F., Beuchle, R., Mayaux, P., Stibig, H.-J., Bodart, C., Brink, A., Carboni, S., Desclée, B., Donnay, F., Eva, H. D., Lupi, A., Raši, R., Seliger, R. and Simonetti, D.: Determination of tropical deforestation rates and related carbon losses from 1990 to 2010, Glob. Change Biol., 20(8), 2540–2554, doi:10.1111/gcb.12605, 2014.

Asner, G. P. and Mascaro, J.: Mapping tropical forest carbon: Calibrating plot estimates to a simple LiDAR metric, Remote Sens. Environ., 140, 614–624, doi:10.1016/j.rse.2013.09.023, 2014.

Asner, G. P., Mascaro, J., Muller-Landau, H. C., Vieilledent, G., Vaudry, R., Rasamoelina, M., Hall, J. S. and van Breugel, M.: A universal airborne LiDAR approach for tropical forest carbon mapping, Oecologia, 168(4), 1147–1160, doi:10.1007/s00442-011-2165-z, 2012.

Asner, G. P., Powell, G. V. N., Mascaro, J., Knapp, D. E., Clark, J. K., Jacobson, J., Kennedy-Bowdoin, T., Balaji, A., Paez-Acosta, G., Victoria, E., Secada, L., Valqui, M. and Hughes, R. F.: High-resolution forest carbon stocks and emissions in the Amazon, Proc. Natl. Acad. Sci., 107(38), 16738–16742, doi:10.1073/pnas.1004875107, 2010.

Baskerville, G. L.: Use of Logarithmic Regression in the Estimation of Plant Biomass., 1972.

Bolton, D. K., Coops, N. C. and Wulder, M. A.: Characterizing residual structure and forest recovery following high-severity fire in the western boreal of Canada using Landsat time-series and airborne lidar data, Remote Sens. Environ., 163, 48–60, doi:10.1016/j.rse.2015.03.004, 2015.

Brockelman, W. Y., Nathalang, A. and Gale, G. A.: The Mo Singto forest dynamics plot, Khao Yai National Park, Thailand, Nat. Hist. Bull. Siam Soc., 57(35–56), 22, 2011.

Brockelman, W. Y., Nathalang, A. and Maxwell, J. F.: Mo Singto Plot: Flora and Ecology, National Science and Technology Development Agency, and Department of National Parks, Wildlife and Plant Conservation, Bangkok., 2017.

Brown, S. and Lugo, A. E.: Tropical secondary forests, J. Trop. Ecol., 6(1), 1–32, doi:10.1017/S0266467400003989, 1990.

Cao, L., Coops, N. C., Innes, J. L., Dai, J., Ruan, H. and She, G.: Tree species classification in subtropical forests using small-footprint full-waveform LiDAR data, Int. J. Appl. Earth Obs. Geoinformation, 49, 39–51, doi:10.1016/j.jag.2016.01.007, 2016.

Chai, F. Y. C.: Above-Ground biomass estimation of a secondary forest in Sarawak, J. Trop. For. Sci., 10, 1997.

Chanthorn, W., Hartig, F. and Brockelman, W. Y.: Structure and community composition in a tropical forest suggest a change of ecological processes during stand development, For. Ecol. Manag., 404, 100–107, doi:10.1016/j.foreco.2017.08.001, 2017.

Chanthorn, W., Ratanapongsai, Y., Brockelman, W. Y., Allen, M. A., Favier, C. and Dubois, M. A.: Viewing tropical forest succession as a three-dimensional dynamical system, Theor. Ecol., 9(2), 163–172, doi:10.1007/s12080-015-0278-4, 2016.

Chave, J., Coomes, D., Jansen, S., Lewis, S. L., Swenson, N. G. and Zanne, A. E.: Towards a worldwide wood economics spectrum, Ecol. Lett., 12(4), 351–366, doi:10.1111/j.1461-0248.2009.01285.x, 2009.

Chave, J., Piponiot, C., Maréchaux, I., Foresta, H. de, Larpin, D., Fischer, F. J., Derroire, G., Vincent, G. and Hérault, B.: Slow rate of secondary forest carbon accumulation in the Guianas compared with the rest of the Neotropics, Ecological Applications, In Press, doi:10.1002/eap.2004, 2019.

Chave, J., Réjou-Méchain, M., Búrquez, A., Chidumayo, E., Colgan, M. S., Delitti, W. B. C., Duque, A., Eid, T., Fearnside, P. M., Goodman, R. C., Henry, M., Martínez-Yrízar, A., Mugasha, W. A., Muller-Landau, H. C., Mencuccini, M., Nelson, B. W., Ngomanda, A., Nogueira, E. M., Ortiz-Malavassi, E., Pélissier, R., Ploton, P., Ryan, C. M., Saldarriaga, J. G. and Vieilledent, G.: Improved allometric models to estimate the aboveground biomass of tropical trees, Glob. Change Biol., 20(10), 3177–3190, doi:10.1111/gcb.12629, 2014.

Chazdon, R. L., Broadbent, E. N., Rozendaal, D. M. A., Bongers, F., Zambrano, A. M. A., Aide, T. M., Balvanera, P., Becknell, J. M., Boukili, V., Brancalion, P. H. S., Craven, D., Almeida-Cortez, J. S., Cabral, G. A. L., de Jong, B., Denslow, J. S., Dent, D. H., DeWalt, S. J., Dupuy, J.

M., Durán, S. M., Espírito-Santo, M. M., Fandino, M. C., César, R. G., Hall, J. S., Hernández-Stefanoni, J. L., Jakovac, C. C., Junqueira, A. B., Kennard, D., Letcher, S. G., Lohbeck, M., Martínez-Ramos, M., Massoca, P., Meave, J. A., Mesquita, R., Mora, F., Muñoz, R., Muscarella, R., Nunes, Y. R. F., Ochoa-Gaona, S., Orihuela-Belmonte, E., Peña-Claros, M., Pérez-García, E. A., Piotto, D., Powers, J. S., Rodríguez-Velazquez, J., Romero-Pérez, I. E., Ruíz, J., Saldarriaga, J. G., Sanchez-Azofeifa, A., Schwartz, N. B., Steininger, M. K., Swenson, N. G., Uriarte, M., van Breugel, M., van der Wal, H., Veloso, M. D. M., Vester, H., Vieira, I. C. G., Bentos, T. V., Williamson, G. B. and Poorter, L.: Carbon sequestration potential of second-growth forest regeneration in the Latin American tropics, Sci. Adv., 2(5), e1501639, doi:10.1126/sciadv.1501639, 2016.

Chazdon, R. L., Letcher, S. G., van Breugel, M., Martínez-Ramos, M., Bongers, F. and Finegan, B.: Rates of change in tree communities of secondary Neotropical forests following major disturbances, Philos. Trans. R. Soc. B Biol. Sci., 362(1478), 273–289, doi:10.1098/rstb.2006.1990, 2007.

Chazdon, R. L.: Second Growth: The Promise of Tropical Forest Regeneration in an Age of Deforestation, University of Chicago Press., 2014.

Cohen, W. B., Harmon, M. E., Wallin, D. O. and Fiorella, M.: Two Decades of Carbon Flux from Forests of the Paci6.c Northwest, , 46(11), 9, 1996.

Coomes, D. A., Dalponte, M., Jucker, T., Asner, G. P., Banin, L. F., Burslem, D. F. R. P., Lewis, S. L., Nilus, R., Phillips, O. L., Phua, M.-H. and Qie, L.: Area-based vs tree-centric approaches to mapping forest carbon in Southeast Asian forests from airborne laser scanning data, Remote Sens. Environ., 194, 77–88, doi:10.1016/j.rse.2017.03.017, 2017.

Cumberlege, P. F. and Cumberlege, V. M. S.: A preliminary list of the orchids of Khao Yai National Park, Nat. Hist. Bull. Siam Soc, (20), 155–182, 1963.

Dubayah, R. O., Sheldon, S. L., Clark, D. B., Hofton, M. A., Blair, J. B., Hurtt, G. C. and Chazdon, R. L.: Estimation of tropical forest height and biomass dynamics using lidar remote sensing at La Selva, Costa Rica, J. Geophys. Res. Biogeosciences, 115(G2), doi:10.1029/2009JG000933, 2010.

Ewel, J. J., Chai, P. and Tsai, L. M.: Biomass and Floristics of three young second-growth forests in Sarawak, Malaysian Forester, 46: 347-364, 19, 1983.

FAO: Global forest resources assessment 2010: terms and definitions. FAO working paper 144/E. Food and Agriculture Organization (FAO) of the United Nations (UN), Rome., 2010.

FAO: The State of Food and Agriculture,Investigating in agriculture for a better future, 2012.

Feldpausch, T. R., Banin, L., Phillips, O. L., Baker, T. R., Lewis, S. L., Quesada, C. A., Affum-Baffoe, K., Arets, E. J. M. M., Berry, N. J., Bird, M., Brondizio, E. S., de Camargo, P., Chave, J., Djagbletey, G., Domingues, T. F., Drescher, M., Fearnside, P. M., França, M. B., Fyllas, N. M., Lopez-Gonzalez, G., Hladik, A., Higuchi, N., Hunter, M. O., Iida, Y., Salim, K. A., Kassim, A. R., Keller, M., Kemp, J., King, D. A., Lovett, J. C., Marimon, B. S., Marimon-Junior, B. H., Lenza, E., Marshall, A. R., Metcalfe, D. J., Mitchard, E. T. A., Moran, E. F., Nelson, B. W., Nilus, R., Nogueira, E. M., Palace, M., Patiño, S., Peh, K. S.-H., Raventos, M. T., Reitsma, J. M., Saiz, G., Schrodt, F., Sonké, B., Taedoumg, H. E., Tan, S., White, L., Wöll, H. and Lloyd, J.: Height-diameter allometry of tropical forest trees, Biogeosciences, 8(5), 1081–1106, doi:10.5194/bg-8-1081-2011, 2011.

Feldpausch, T. R., Lloyd, J., Lewis, S. L., Brienen, R. J. W., Gloor, M., Monteagudo Mendoza, A., Lopez-Gonzalez, G., Banin, L., Abu Salim, K., Affum-Baffoe, K., Alexiades, M., Almeida, S., Amaral, I., Andrade, A., Aragão, L. E. O. C., Araujo Murakami, A., Arets, E. J. M. M., Arroyo, L., Aymard C., G. A., Baker, T. R., Bánki, O. S., Berry, N. J., Cardozo, N., Chave, J., Comiskey, J. A., Alvarez, E., de Oliveira, A., Di Fiore, A., Djagbletey, G., Domingues, T. F., Erwin, T. L., Fearnside, P. M., França, M. B., Freitas, M. A., Higuchi, N., E. Honorio C., Iida, Y., Jiménez, E., Kassim, A. R., Killeen, T. J., Laurance, W. F., Lovett, J. C., Malhi, Y., Marimon, B. S., Marimon-Junior, B. H., Lenza, E., Marshall, A. R., Mendoza, C., Metcalfe, D. J., Mitchard, E. T. A., Neill, D. A., Nelson, B. W., Nilus, R., Nogueira, E. M., Parada, A., Peh, K. S.-H., Pena Cruz, A., Peñuela, M. C., Pitman, N. C. A., Prieto, A., Quesada, C. A., Ramírez, F., Ramírez-Angulo, H., Reitsma, J. M., Rudas, A., Saiz, G., Salomão, R. P., Schwarz, M., Silva, N., Silva-Espejo, J. E., Silveira, M., Sonké, B., Stropp, J., Taedoumg, H. E., Tan, S., ter Steege, H., Terborgh, J., Torello-Raventos, M., van der Heijden, G. M. F., Vásquez, R., Vilanova, E., Vos, V. A., White, L., Willcock, S., Woell, H. and Phillips, O. L.: Tree height integrated into pantropical forest biomass estimates, Biogeosciences, 9(8), 3381–3403, doi:10.5194/bg-9-3381-2012, 2012.

Feldpausch, T. R., Prates-Clark, C. da C., Fernandes, E. C. M. and Riha, S. J.: Secondary forest growth deviation from chronosequence predictions in central Amazonia, Glob. Change Biol., 13(5), 967–979, doi:10.1111/j.1365-2486.2007.01344.x, 2007.

Ferraz, A., Saatchi, S., Xu, L., Hagen, S., Chave, J., Yu, Y., Meyer, V., Garcia, M., Silva, C., Roswintiart, O., Samboko, A., Sist, P., Walker, S., Pearson, T. R. H., Wijaya, A., Sullivan, F. B., Rutishauser, E., Hoekman, D. and Ganguly, S.: Carbon storage potential in degraded forests of Kalimantan, Indonesia, Environ. Res. Lett., 13(9), 095001, doi:10.1088/1748-9326/aad782, 2018.

Gibbs, H. K., Brown, S., Niles, J. O. and Foley, J. A.: Monitoring and estimating tropical forest carbon stocks: making REDD a reality, Environ. Res. Lett., 2(4), 045023, doi:10.1088/1748-9326/2/4/045023, 2007.

Goetz, S. J., Baccini, A., Laporte, N. T., Johns, T., Walker, W., Kellndorfer, J., Houghton, R. A. and Sun, M.: Mapping and monitoring carbon stocks with satellite observations: a comparison of methods, Carbon Balance Manag., 4(1), 2, doi:10.1186/1750-0680-4-2, 2009.

Hansen, M. C., Potapov, P. V., Moore, R., Hancher, M., Turubanova, S. A., Tyukavina, A., Thau, D., Stehman, S. V., Goetz, S. J., Loveland, T. R., Kommareddy, A., Egorov, A., Chini, L., Justice, C. O. and Townshend, J. R. G.: High-Resolution Global Maps of 21st-Century Forest Cover Change, Science, 342(6160), 850–853, doi:10.1126/science.1244693, 2013.

Harris, N. L., Brown, S., Hagen, S. C., Saatchi, S. S., Petrova, S., Salas, W., Hansen, M. C., Potapov, P. V. and Lotsch, A.: Baseline Map of Carbon Emissions from Deforestation in Tropical Regions, Science, 336(6088), 1573–1576, doi:10.1126/science.1217962, 2012.

Helmer, E. H., Lefsky, M. A. and Roberts, D. A.: Biomass accumulation rates of Amazonian secondary forest and biomass of old-growth forests from Landsat time series and the Geoscience Laser Altimeter System, J. Appl. Remote Sens. Vol 3 033505 2009, 3(033505), 1–31, doi:10.1117/1.3082116, 2009.

Hiratsuka, M., Toma, T., Diana, R., Hadriyanto, D. and Morikawa, Y.: Biomass Recovery of Naturally Regenerated Vegetation after the 1998 Forest Fire in East Kalimantan, Indonesia, Japan Agricultural Research Quarterly: JARQ, 40(3), 277–282, doi:10.6090/jarq.40.277, 2006.

IPCC: Guidelines for national greenhouse gas inventories, Agriculture, Forestry and other land use (AFLOLU), Institute for Global Environmental strategies, Hayama, Japan, vol. 4, 2006., 2006.

Jepsen, M. R.: Above-ground carbon stocks in tropical fallows, Sarawak, Malaysia, For. Ecol. Manag., 225(1), 287–295, doi:10.1016/j.foreco.2006.01.005, 2006.

Jucker, T., Asner, G. P., Dalponte, M., Brodrick, P. G., Philipson, C. D., Vaughn, N. R., Teh, Y. A., Brelsford, C., Burslem, D. F. R. P., Deere, N. J., Ewers, R. M., Kvasnica, J., Lewis, S. L., Malhi, Y., Milne, S., Nilus, R., Pfeifer, M., Phillips, O. L., Qie, L., Renneboog, N., Reynolds, G., Riutta, T., Struebig, M. J., Svátek, M., Turner, E. C. and Coomes, D. A.: Estimating aboveground carbon density and its uncertainty in Borneo's structurally complex tropical forests using airborne laser scanning, Biogeosciences, 15(12), 3811–3830, doi:10.5194/bg-15-3811-2018, 2018.

Jucker, T., Asner, G. P., Dalponte, M., Brodrick, P., Vaughn, N., Brelsford, C., Ewers, R. M., Kvasnica, J., Lewis, S. L., Malhi, Y., Milne, S., Nilus, R., Pfeifer, M., Phillips, O., Qie, L., Renneboog, N., Riutta, T., Struebig, M. J., Svátek, M., Teh, Y. A. and Coomes, D. A.: A regional model for estimating the aboveground carbon density of Borneo's tropical forests from airborne laser scanning, , 72, 2017.

Junttila, V., Kauranne, T., Finley, A. O. and Bradford, J. B.: Linear Models for Airborne-Laser-Scanning-Based Operational Forest Inventory With Small Field Sample Size and Highly Correlated LiDAR Data, IEEE Trans. Geosci. Remote Sens., 53(10), 5600–5612, doi:10.1109/TGRS.2015.2425916, 2015.

Kennard, D. K., Gould, K., Putz, F. E., Fredericksen, T. S. and Morales, F.: Effect of disturbance intensity on regeneration mechanisms in a tropical dry forest, For. Ecol. Manag., 162(2), 197–208, doi:10.1016/S0378-1127(01)00506-0, 2002.

Kitamura, S., Yumoto, T., Poonswad, P., Chuailua, P. and Plongmai, K.: Characteristics of hornbill-dispersed fruits in a tropical seasonal forest in Thailand, Bird Conserv. Int., 14(S1), S81–S88, doi:10.1017/S0959270905000250, 2004.

Kronseder, K., Ballhorn, U., Böhm, V. and Siegert, F.: Above ground biomass estimation across forest types at different degradation levels in Central Kalimantan using LiDAR data, Int. J. Appl. Earth Obs. Geoinformation, 18, 37–48, doi:10.1016/j.jag.2012.01.010, 2012.

Labriere, N., Tao, S., Chave, J., Scipal, K., Toan, T. L., Abernethy, K., Alonso, A., Barbier, N., Bissiengou, P., Casal, T., Davies, S. J., Ferraz, A., Herault, B., Jaouen, G., Jeffery, K. J., Kenfack, D., Korte, L., Lewis, S. L., Malhi, Y., Memiaghe, H. R., Poulsen, J. R., Rejou-Mechain, M., Villard, L., Vincent, G., White, L. J. T. and Saatchi, S.: In Situ Reference Datasets From the TropiSAR and AfriSAR Campaigns in Support of Upcoming Spaceborne Biomass Missions, IEEE J. Sel. Top. Appl. Earth Obs. Remote Sens., 11(10), 3617–3627, doi:10.1109/JSTARS.2018.2851606, 2018.

Letcher, S. G. and Chazdon, R. L.: Rapid Recovery of Biomass, Species Richness, and Species Composition in a Forest Chronosequence in Northeastern Costa Rica - Letcher - 2009 - Biotropica - Wiley Online Library, [online] Available from: https://onlinelibrary.wiley.com/doi/epdf/10.1111/j.1744-7429.2009.00517.x (Accessed 20 June 2019), 2009.

Liaw, A. and Wiener, M.: Classification and Regression by randomForest, , 2, 6, 2002.

Lohbeck, M., Poorter, L., Martínez-Ramos, M. and Bongers, F.: Biomass is the main driver of changes in ecosystem process rates during tropical forest succession, Ecology, 96(5), 1242–1252, doi:10.1890/14-0472.1, 2015.

Losos, E. C. and Leigh, E. G.: Tropical forest diversity and dynamism, University of Chicago Press. [online] Available from: http://agris.fao.org/agris-search/search.do?recordID=US201300095159 (Accessed 20 June 2019), 2004.

Lu, D.: The potential and challenge of remote sensing-based biomass estimation, Int. J. Remote Sens., 27(7), 1297–1328, doi:10.1080/01431160500486732, 2006.

Lugo, A. E. and Brown, S.: Tropical forests as sinks of atmospheric carbon, For. Ecol. Manag., 54(1–4), 239–255, doi:10.1016/0378-1127(92)90016-3, 1992.

Maltamo, M., Packalén, P., Yu, X., Eerikäinen, K., Hyyppä, J. and Pitkänen, J.: Identifying and quantifying structural characteristics of heterogeneous boreal forests using laser scanner data, For. Ecol. Manag., 216(1), 41–50, doi:10.1016/j.foreco.2005.05.034, 2005.

Masek, J. G. and Collatz, G. J.: Estimating forest carbon fluxes in a disturbed southeastern landscape: Integration of remote sensing, forest inventory, and biogeochemical modeling, J. Geophys. Res., 111(G1), G01006, doi:10.1029/2005JG000062, 2006.

McMahon, S. M., Arellano, G. and Davies, S. J.: The importance and challenges of detecting changes in forest mortality rates, Ecosphere, 10(2), e02615, doi:10.1002/ecs2.2615, 2019.

Meyer, V., Saatchi, S. S., Chave, J., Dalling, J. W., Bohlman, S., Fricker, G. A., Robinson, C., Neumann, M. and Hubbell, S.: Detecting tropical forest biomass dynamics from repeated airborne lidar measurements, Biogeosciences, 10(8), 5421–5438, doi:10.5194/bg-10-5421-2013, 2013.

Meyer, V., Saatchi, S., Ferraz, A., Xu, L., Duque, A., García, M. and Chave, J.: Forest degradation and biomass loss along the Chocó region of Colombia, Carbon Balance Manag., 14(1), 2, doi:10.1186/s13021-019-0117-9, 2019.

Mitchard, E. T. A., Feldpausch, T. R., Brienen, R. J. W., Lopez-Gonzalez, G., Monteagudo, A., Baker, T. R., Lewis, S. L., Lloyd, J., Quesada, C. A., Gloor, M., Steege, H. ter, Meir, P., Alvarez, E., Araujo-Murakami, A., Aragão, L. E. O. C., Arroyo, L., Aymard, G., Banki, O., Bonal, D., Brown, S., Brown, F. I., Cerón, C. E., Moscoso, V. C., Chave, J., Comiskey, J. A., Cornejo, F., Medina, M. C., Costa, L. D., Costa, F. R. C., Fiore, A. D., Domingues, T. F., Erwin, T. L., Frederickson, T., Higuchi, N., Coronado, E. N. H., Killeen, T. J., Laurance, W. F., Levis, C., Magnusson, W. E., Marimon, B. S., Junior, B. H. M., Polo, I. M., Mishra, P., Nascimento, M. T., Neill, D., Vargas, M. P. N., Palacios, W. A., Parada, A., Molina, G. P., Peña-Claros, M., Pitman, N., Peres, C. A., Poorter, L., Prieto, A., Ramirez-Angulo, H., Correa, Z. R., Roopsind, A., Roucoux, K. H., Rudas, A., Salomão, R. P., Schietti, J., Silveira, M., Souza, P. F. de, Steininger, M. K., Stropp, J., Terborgh, J., Thomas, R., Toledo, M., Torres-Lezama, A., Andel, T. R. van, Heijden, G. M. F. van der, Vieira, I. C. G., Vieira, S., Vilanova-Torre, E., Vos, V. A., Wang, O., Zartman, C. E., Malhi, Y. and Phillips, O. L.: Markedly divergent estimates of Amazon forest carbon density from ground plots and satellites, Glob. Ecol. Biogeogr., 23(8), 935–946, doi:10.1111/geb.12168, 2014.

Mitchard, E. T., Saatchi, S. S., Baccini, A., Asner, G. P., Goetz, S. J., Harris, N. L. and Brown, S.: Uncertainty in the spatial distribution of tropical forest biomass: a comparison of pan-tropical maps, Carbon Balance Manag., 8(1), 10, doi:10.1186/1750-0680-8-10, 2013.

N'Guessan, A. E., N'dja, J. K., Yao, O. N., Amani, B. H. K., Gouli, R. G. Z., Piponiot, C., Zo-Bi, I. C. and Hérault, B.: Drivers of biomass recovery in a secondary forested landscape of West Africa, For. Ecol. Manag., 433, 325–331, doi:10.1016/j.foreco.2018.11.021, 2019.

Næsset, E.: Predicting forest stand characteristics with airborne scanning laser using a practical two-stage procedure and field data, Remote Sens. Environ., 80(1), 88–99, doi:10.1016/S0034-4257(01)00290-5, 2002.

Norden, N., Angarita, H. A., Bongers, F., Martínez-Ramos, M., Granzow-de la Cerda, I., van Breugel, M., Lebrija-Trejos, E., Meave, J. A., Vandermeer, J., Williamson, G. B., Finegan, B., Mesquita, R. and Chazdon, R. L.: Successional dynamics in Neotropical forests are as uncertain as they are predictable, Proc. Natl. Acad. Sci., 112(26), 8013–8018, doi:10.1073/pnas.1500403112, 2015.

Norden, N., Mesquita, R. C. G., Bentos, T. V., Chazdon, R. L. and Williamson, G. B.: Contrasting community compensatory trends in alternative successional pathways in central Amazonia, Oikos, 120(1), 143–151, doi:10.1111/j.1600-0706.2010.18335.x, 2011.

Oliver, C. D. and Larson, B. C.: Forest stand dynamics, New York: Wiley., 520, 1996.

Pflugmacher, D., Cohen, W. B. and E. Kennedy, R.: Using Landsat-derived disturbance history (1972–2010) to predict current forest structure, Remote Sens. Environ., 122, 146–165, doi:10.1016/j.rse.2011.09.025, 2012.

Pflugmacher, D., Cohen, W. B., Kennedy, R. E. and Yang, Z.: Using Landsat-derived disturbance and recovery history and lidar to map forest biomass dynamics, Remote Sens. Environ., 151, 124–137, doi:10.1016/j.rse.2013.05.033, 2014.

Pickell, P. D., Hermosilla, T., Frazier, R. J., Coops, N. C. and Wulder, M. A.: Forest recovery trends derived from Landsat time series for North American boreal forests, Int. J. Remote Sens., 37(1), 138–149, doi:10.1080/2150704X.2015.1126375, 2016.

Poorter, L., Bongers, F., Aide, T. M., Almeyda Zambrano, A. M., Balvanera, P., Becknell, J. M., Boukili, V., Brancalion, P. H. S., Broadbent, E. N., Chazdon, R. L., Craven, D., de Almeida-Cortez, J. S., Cabral, G. A. L., de Jong, B. H. J., Denslow, J. S., Dent, D. H., DeWalt, S. J., Dupuy, J. M., Durán, S. M., Espírito-Santo, M. M., Fandino, M. C., César, R. G., Hall, J. S., Hernandez-Stefanoni, J. L., Jakovac, C. C., Junqueira, A. B., Kennard, D., Letcher, S. G., Licona, J.-C., Lohbeck, M., Marín-Spiotta, E., Martínez-Ramos, M., Massoca, P., Meave, J. A., Mesquita, R., Mora, F., Muñoz, R., Muscarella, R., Nunes, Y. R. F., Ochoa-Gaona, S., de Oliveira, A. A., Orihuela-Belmonte, E., Peña-Claros, M., Pérez-García, E. A., Piotto, D., Powers, J. S., Rodríguez-Velázquez, J., Romero-Pérez, I. E., Ruíz, J., Saldarriaga, J. G., Sanchez-Azofeifa, A., Schwartz, N. B., Steininger, M. K., Swenson, N. G., Toledo, M., Uriarte, M., van Breugel, M., van der Wal, H., Veloso, M. D. M., Vester, H. F. M., Vicentini, A., Vieira, I. C. G., Bentos, T. V., Williamson, G. B. and Rozendaal, D. M. A.: Biomass resilience of Neotropical secondary forests, Nature, 530(7589), 211–214, doi:10.1038/nature16512, 2016a.

Poorter, L., Bongers, F., Aide, T. M., Almeyda Zambrano, A. M., Balvanera, P., Becknell, J. M., Boukili, V., Brancalion, P. H. S., Broadbent, E. N., Chazdon, R. L., Craven, D., de Almeida-Cortez, J. S., Cabral, G. A. L., de Jong, B. H. J., Denslow, J. S., Dent, D. H., DeWalt, S. J., Dupuy, J. M., Durán, S. M., Espírito-Santo, M. M., Fandino, M. C., César, R. G., Hall, J. S., Hernandez-Stefanoni, J. L., Jakovac, C. C., Junqueira, A. B., Kennard, D., Letcher, S. G., Licona, J.-C., Lohbeck, M., Marín-Spiotta, E., Martínez-Ramos, M., Massoca, P., Meave, J. A., Mesquita, R., Mora, F., Muñoz, R., Muscarella, R., Nunes, Y. R. F., Ochoa-Gaona, S., de Oliveira, A. A., Orihuela-Belmonte, E., Peña-Claros, M., Pérez-García, E. A., Piotto, D., Powers, J. S., Rodríguez-Velázquez, J., Romero-Pérez, I. E., Ruíz, J., Saldarriaga, J. G., Sanchez-Azofeifa, A., Schwartz, N. B., Steininger, M. K., Swenson, N. G., Toledo, M., Uriarte, M., van Breugel, M., van der Wal, H., Veloso, M. D. M., Vester, H. F. M., Vicentini, A., Vieira, I. C. G., Vizcarra Bentos, T., Williamson, G. B. and Rozendaal, D. M. A.: Data from: Biomass resilience of Neotropical secondary forests, , doi:10.5061/dryad.82vr4, 2016b.

Ray, G. J. and Brown, B. J.: Seed Ecology of Woody Species in a Caribbean Dry Forest, Restor. Ecol., 2, 156–163, doi:10.1111/j.1526-100X.1994.tb00063.x, 2006.

Réjou-Méchain, M., Barbier, N., Couteron, P., Ploton, P., Vincent, G., Herold, M., Mermoz, S., Saatchi, S., Chave, J., de Boissieu, F., Féret, J.-B., Takoudjou, S. M. and Pélissier, R.: Upscaling

Forest Biomass from Field to Satellite Measurements: Sources of Errors and Ways to Reduce Them, Surv. Geophys., doi:10.1007/s10712-019-09532-0, 2019.

Réjou-Méchain, M., Tanguy, A., Piponiot, C., Chave, J. and Hérault, B.: biomass: an r package for estimating above-ground biomass and its uncertainty in tropical forests, Methods Ecol. Evol., 8(9), 1163–1167, doi:10.1111/2041-210X.12753, 2017.

Réjou-Méchain, M., Tymen, B., Blanc, L., Fauset, S., Feldpausch, T. R., Monteagudo, A., Phillips, O. L., Richard, H. and Chave, J.: Using repeated small-footprint LiDAR acquisitions to infer spatial and temporal variations of a high-biomass Neotropical forest, Remote Sens. Environ., 169, 93–101, doi:10.1016/j.rse.2015.08.001, 2015.

Requena Suarez, D., Rozendaal, D. M. A., De Sy, V., Phillips, O. L., Alvarez-Dávila, E., Anderson-Teixeira, K., Araujo-Murakami, A., Arroyo, L., Baker, T. R., Bongers, F., Brienen, R. J. W., Carter, S., Cook-Patton, S. C., Feldpausch, T. R., Griscom, B. W., Harris, N., Hérault, B., Honorio Coronado, E. N., Leavitt, S. M., Lewis, S. L., Marimon, B. S., Monteagudo Mendoza, A., Kassi N'dja, J., N'Guessan, A. E., Poorter, L., Qie, L., Rutishauser, E., Sist, P., Sonké, B., Sullivan, M. J. P., Vilanova, E., Wang, M. M. H., Martius, C. and Herold, M.: Estimating aboveground net biomass change for tropical and subtropical forests: Refinement of IPCC default rates using forest plot data, Glob Chang Biol, 25(11), 3609–3624, doi:10.1111/gcb.14767, 2019.

Roussel, J.-R. and Auty, D.: lidR: Airborne LiDAR Data Manipulation and Visualization for Forestry Applications., 2017.

Rozendaal, D. M. A. and Chazdon, R. L.: Demographic drivers of tree biomass change during secondary succession in northeastern Costa Rica, Ecol. Appl., 25(2), 506–516, doi:10.1890/14-0054.1, 2015.

Rozendaal, D. M. A., Chazdon, R. L., Arreola-Villa, F., Balvanera, P., Bentos, T. V., Dupuy, J. M., Hernández-Stefanoni, J. L., Jakovac, C. C., Lebrija-Trejos, E. E., Lohbeck, M., Martínez-Ramos, M., Massoca, P. E. S., Meave, J. A., Mesquita, R. C. G., Mora, F., Pérez-García, E. A., Romero-Pérez, I. E., Saenz-Pedroza, I., van Breugel, M., Williamson, G. B. and Bongers, F.: Demographic Drivers of Aboveground Biomass Dynamics During Secondary Succession in Neotropical Dry and Wet Forests, Ecosystems, 20(2), 340–353, doi:10.1007/s10021-016-0029-4, 2017.

Ruiz, J., Fandino, M. C. and Chazdon, R. L.: Vegetation Structure, Composition, and Species Richness Across a 56-year Chronosequence of Dry Tropical Forest on Providencia Island, Colombia1, Biotropica, 37(4), 520–530, doi:10.1111/j.1744-7429.2005.00070.x, 2005.

Saldarriaga, J. G., West, D. C., Tharp, M. L. and Uhl, C.: Long-Term Chronosequence of Forest Succession in the Upper Rio Negro of Colombia and Venezuela, J. Ecol., 76(4), 938–958, doi:10.2307/2260625, 1988.

Sasaki, N. and Putz, F. E.: Critical need for new definitions of “forest” and “forest degradation” in global climate change agreements, Conserv. Lett., 2(5), 226–232, doi:10.1111/j.1755-263X.2009.00067.x, 2009.

Silver, W. L., Ostertag, R. and Lugo, A. E.: The Potential for Carbon Sequestration Through Reforestation of Abandoned Tropical Agricultural and Pasture Lands, Restor. Ecol., 8(4), 394–407, doi:10.1046/j.1526-100x.2000.80054.x, 2000.

Smitinand, T.: Vegetation of Khao Yai National Park, Siam Society, 1968.

Stas, S. M., Rutishauser, E., Chave, J., Anten, N. P. R. and Laumonier, Y.: Estimating the aboveground biomass in an old secondary forest on limestone in the Moluccas, Indonesia: Comparing locally developed versus existing allometric models, For. Ecol. Manag., 389, 27–34, doi:10.1016/j.foreco.2016.12.010, 2017.

Stibig, H.-J., Achard, F., Carboni, S., Raši, R. and Miettinen, J.: Change in tropical forest cover of Southeast Asia from 1990 to 2010, Biogeosciences, 11(2), 247–258, doi:https://doi.org/10.5194/bg-11-247-2014, 2014.

Sullivan, M. J. P., Talbot, J., Lewis, S. L., Phillips, O. L., Qie, L., Begne, S. K., Chave, J., Cuni-Sanchez, A., Hubau, W., Lopez-Gonzalez, G., Miles, L., Monteagudo-Mendoza, A., Sonké, B., Sunderland, T., ter Steege, H., White, L. J. T., Affum-Baffoe, K., Aiba, S., de Almeida, E. C., de Oliveira, E. A., Alvarez-Loayza, P., Dávila, E. Á., Andrade, A., Aragão, L. E. O. C., Ashton, P., C, G. A. A., Baker, T. R., Balinga, M., Banin, L. F., Baraloto, C., Bastin, J.-F., Berry, N., Bogaert, J., Bonal, D., Bongers, F., Brienen, R., Camargo, J. L. C., Cerón, C., Moscoso, V. C., Chezeaux, E., Clark, C. J., Pacheco, Á. C., Comiskey, J. A., Valverde, F. C., Coronado, E. N. H., Dargie, G., Davies, S. J., De Canniere, C., K, M. N. D., Doucet, J.-L., Erwin, T. L., Espejo, J. S., Ewango, C. E. N., Fauset, S., Feldpausch, T. R., Herrera, R., Gilpin, M., Gloor, E., Hall, J. S., Harris, D. J., Hart, T. B., Kartawinata, K., Kho, L. K., Kitayama, K., Laurance, S. G. W., Laurance, W. F., Leal, M. E., Lovejoy, T., Lovett, J. C., Lukasu, F. M., Makana, J.-R., Malhi, Y., Maracahipes, L., Marimon, B. S., Junior, B. H. M., Marshall, A. R., Morandi, P. S., Mukendi, J. T., Mukinzi, J., Nilus, R., Vargas, P. N., Camacho, N. C. P., Pardo, G., Peña-Claros, M., Pétronelli, P., Pickavance, G. C., Poulsen, A. D., Poulsen, J. R., Primack, R. B., Priyadi, H., Quesada, C. A., Reitsma, J., Réjou-Méchain, M., Restrepo, Z., Rutishauser, E., Salim, K. A., Salomão, R. P., Samsoedin, I., Sheil, D., et al.: Diversity and carbon storage across the tropical forest biome, Sci. Rep., 7, 39102, doi:10.1038/srep39102, 2017.

Thomas, S. C. and Martin, A. R.: Carbon Content of Tree Tissues: A Synthesis, Forests, 3(2), 332–352, doi:10.3390/f3020332, 2012.

Toledo, M. and Salick, J.: Secondary Succession and Indigenous Management in Semideciduous Forest Fallows of the Amazon Basin [1]: Secondary Succession and Indigenous Management, Biotropica, 38(2), 161–170, doi:10.1111/j.1744-7429.2006.00120.x, 2006.

White, J. C., Saarinen, N., Kankare, V., Wulder, M. A., Hermosilla, T., Coops, N. C., Pickell, P. D., Holopainen, M., Hyyppä, J. and Vastaranta, M.: Confirmation of post-harvest spectral recovery from Landsat time series using measures of forest cover and height derived from airborne laser scanning data, Remote Sens. Environ., 216, 262–275, doi:10.1016/j.rse.2018.07.004, 2018.

Wulder, M. A., White, J. C., Bater, C. W., Coops, N. C., Hopkinson, C. and Chen, G.: Lidar plots — a new large-area data collection option: context, concepts, and case study, Can. J. Remote Sens., 38(5), 600–618, doi:10.5589/m12-049, 2012.

Zald, H. S. J., Ohmann, J. L., Roberts, H. M., Gregory, M. J., Henderson, E. B., McGaughey, R. J. and Braaten, J.: Influence of lidar, Landsat imagery, disturbance history, plot location accuracy, and plot size on accuracy of imputation maps of forest composition and structure, Remote Sens. Environ., 143, 26–38, doi:10.1016/j.rse.2013.12.013, 2014.

Zanne, A. E., Lopez-Gonzalez, G., Coomes, D. A., Ilic, J., Jansen, S., Lewis, S. L., Miller, R. B., Swenson, N. G., Wiemann, M. C. and Chave, J.: Data from: Towards a worldwide wood economics spectrum, , doi:10.5061/dryad.234, 2009.

Zhao, K., Popescu, S. and Nelson, R.: Lidar remote sensing of forest biomass: A scale-invariant estimation approach using airborne lasers, Remote Sens. Environ., 113(1), 182–196, doi:10.1016/j.rse.2008.09.009, 2009.

Zheng, D., Rademacher, J., Chen, J., Crow, T., Bresee, M., Le Moine, J. and Ryu, S.-R.: Estimating aboveground biomass using Landsat 7 ETM+ data across a managed landscape in northern Wisconsin, USA, Remote Sens. Environ., 93(3), 402–411, doi:10.1016/j.rse.2004.08.008, 2004.

Zolkos, S. G., Goetz, S. J. and Dubayah, R.: A meta-analysis of terrestrial aboveground biomass estimation using lidar remote sensing, Remote Sens. Environ., 128, 289–298, doi:10.1016/j.rse.2012.10.017, 2013.

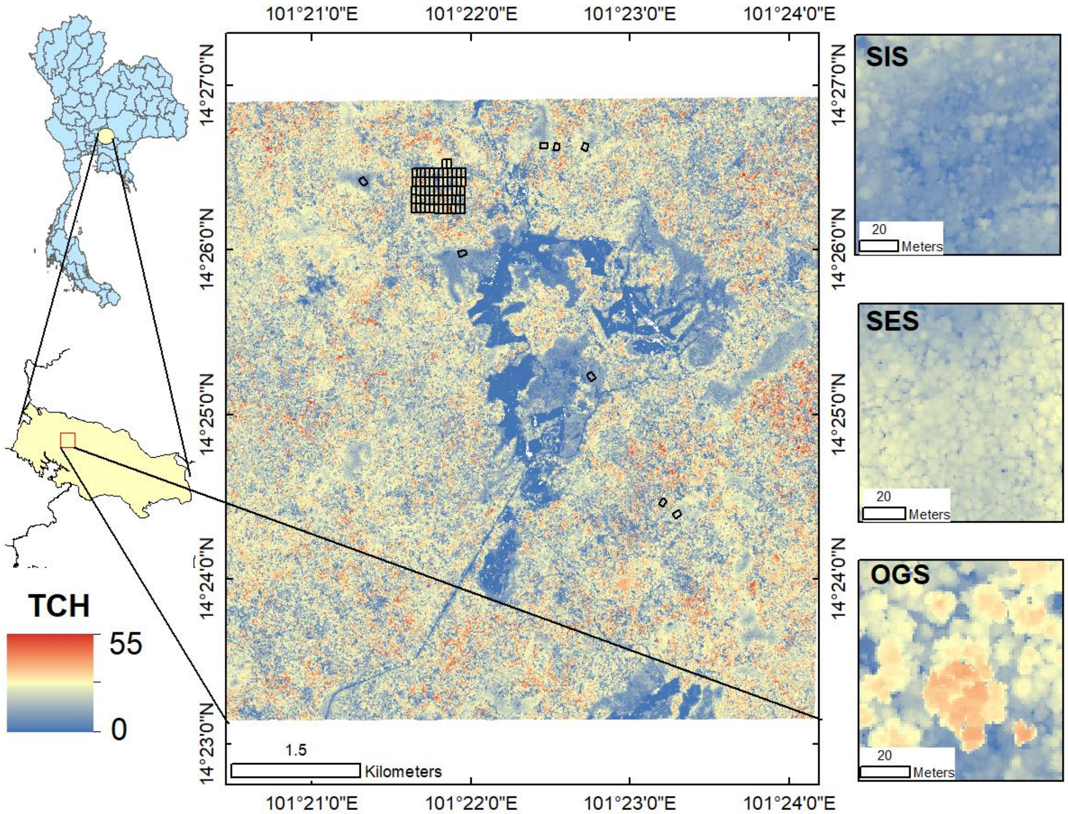

Figure 1. ~~Study area.~~ Location of the study area in Thailand (upper left) and in the Khao Yai reserve (bottom left). The central map illustrates the LiDAR top of canopy height (TCH) in the study area at 1-m resolution and the location of the 70 studied plots (in black). Examples of the different stand development stages are illustrated (right; SIS: stand initiation stage; SES: stem exclusion stage; and OGS: old growth stage).

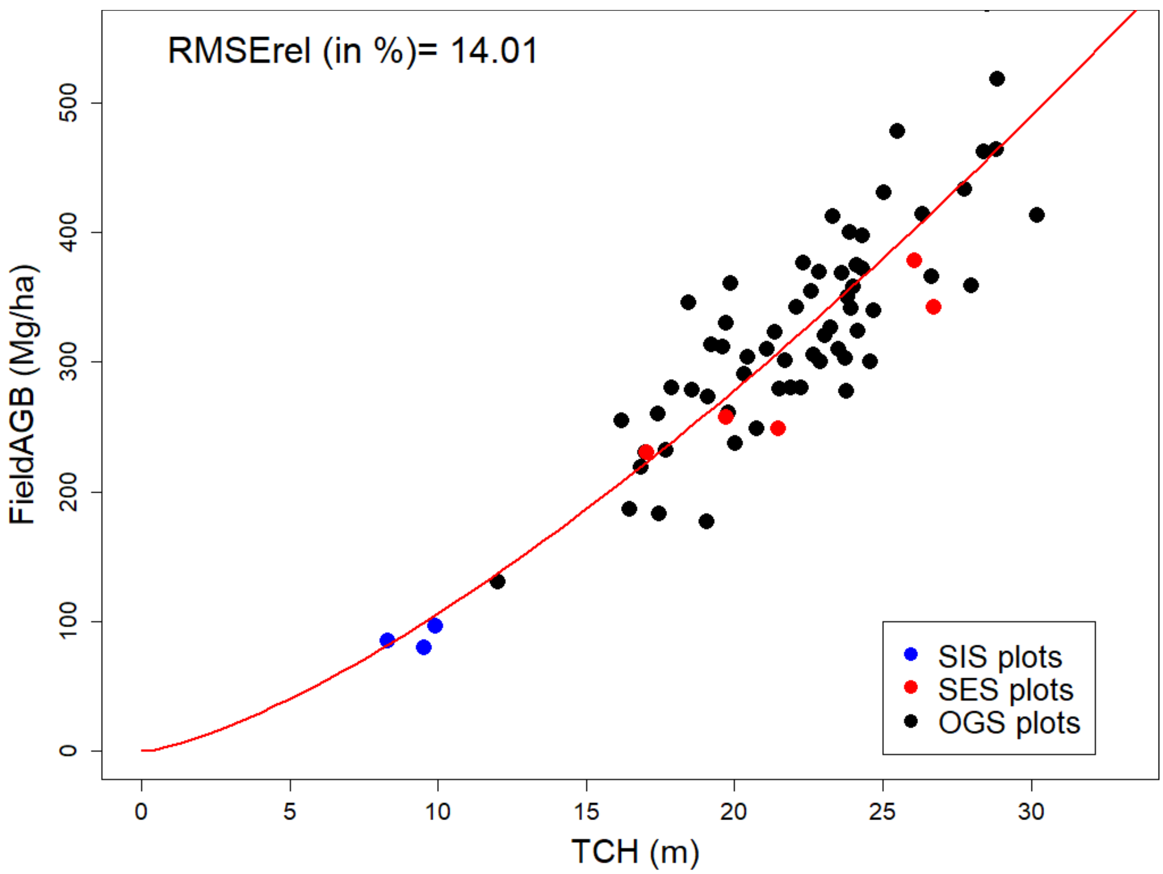

Figure 2. LiDAR-AGB model showing the relationship between field-derived plot AGB and the LiDAR top-of-canopy height (TCH) at a 0.5-ha resolution. The power model is illustrated by the red line, and the point represent the field plot AGB estimates at different successional stages stand initiation (early) stage (SIS; n = 3); stem exclusion (intermediate) stage (SES; n = 5), and old growth stage (OGS; n = 62)according to the classification by Chanthorn et al. (2017).

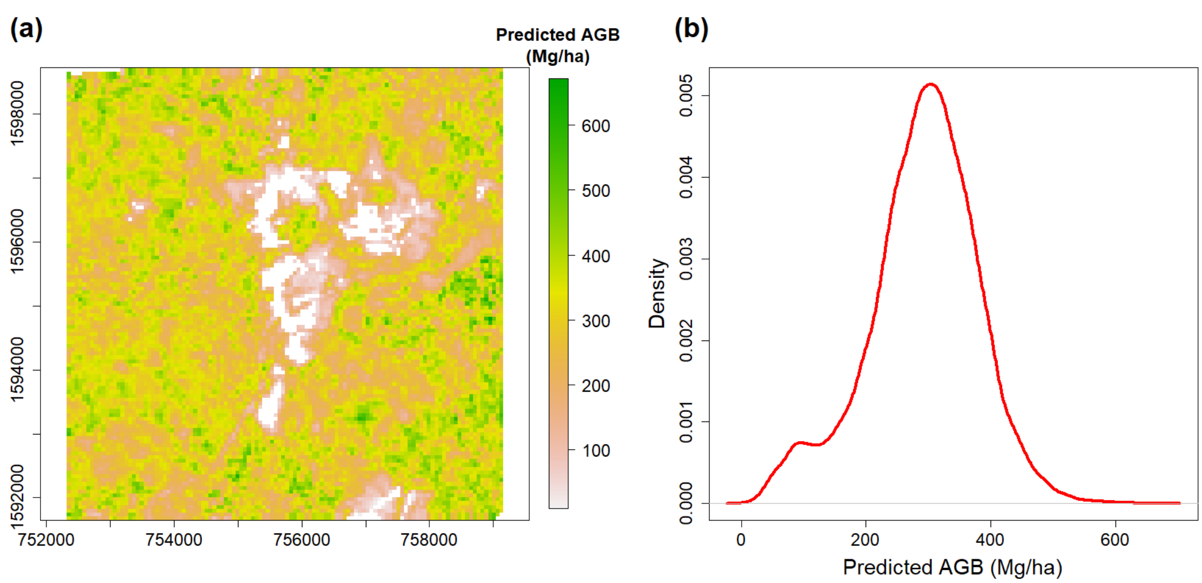

Figure 3. LiDAR-AGB map and the distribution of AGB values over the landscape at 60-m resolution. (a)- Spatial distribution of AGB predicted from the LiDAR-AGB inversion model over the study area; (b)- Density distribution of predicted AGB over the landscape.

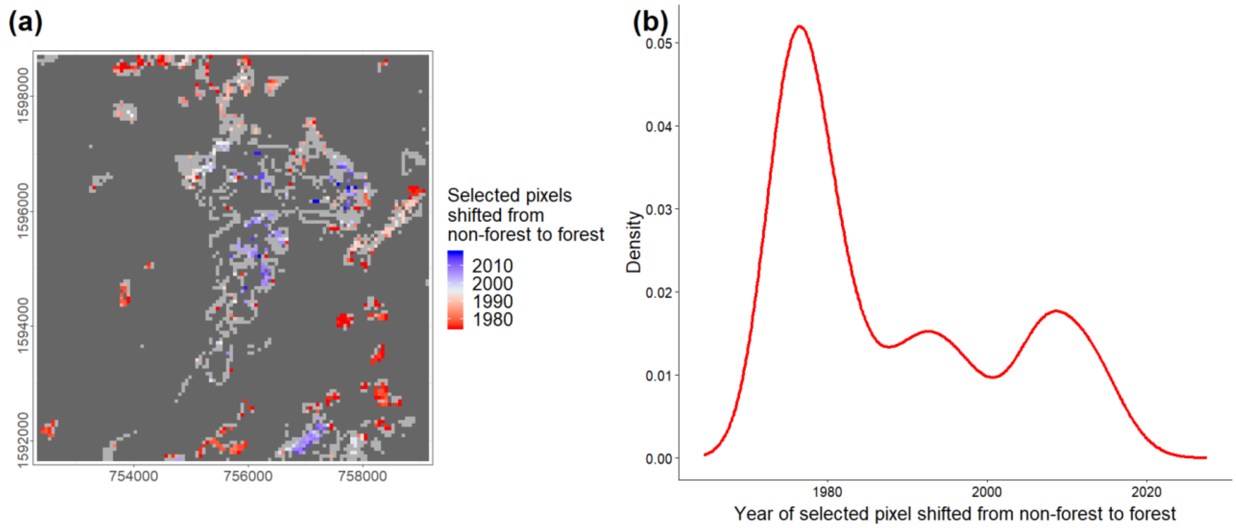

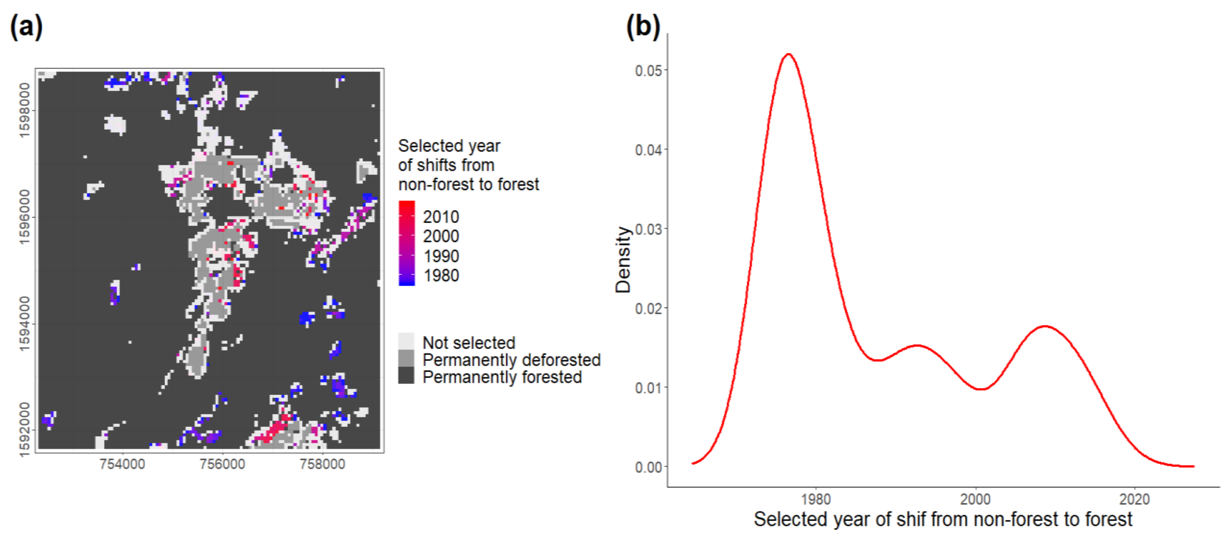

Figure 4. Landsat time series derived map showing non-forest-to-forest change over the study area. (a)- Map showing spatialized selected pixel shifts from non-forests to forests over years. The shade gradient represents pixels that did not experience any shift (permanently forested or permanently deforested) and pixels that experienced a shift but that did not pass our quality procedure during the study period (Not selected) (b)- Density distribution of selected pixel shifts over the landscape during the study period.

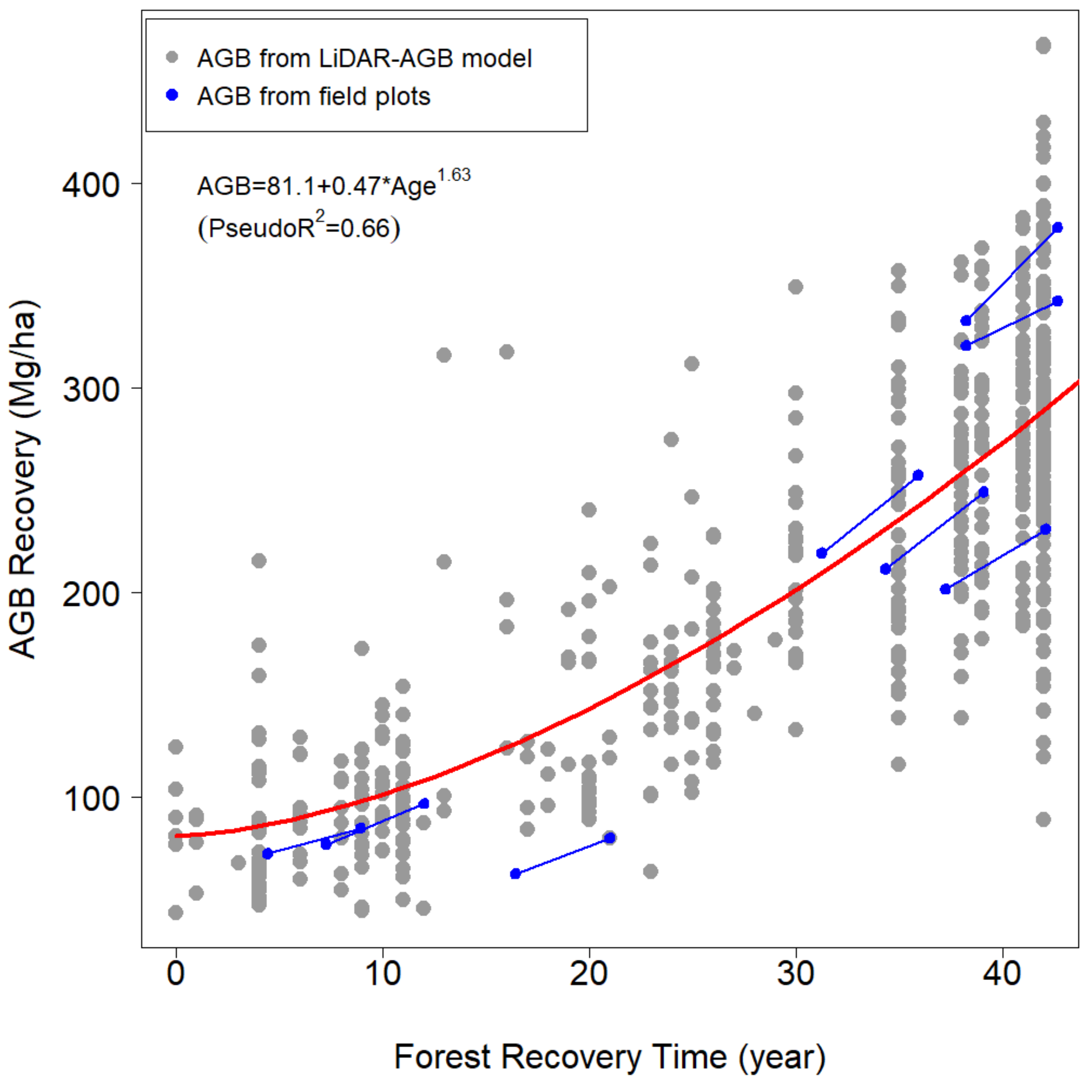

Figure 5. Relationship between forest biomass estimated from a LiDAR-AGB model and forest recovery time estimated from a time series of classified Landsat images (grey dots). The fitted power model is represented by the red line. Blue lines and dots represent the AGB directly estimated from eight field plots (same plots are joined by a line) in 2013 and in 2017/8 and for which the forest recovery time was inferred from Landsat derived forest age (Fig. S5).

Supporting Information for

"Forest aboveground biomass stock and resilience in a tropical landscape of Thailand."

Authors: Nidhi Jha, Nitin Kumar Tripathi, Wirong Chanthorn, Warren Brockelman, Anuttara Nataland, Raphaël Pélissier, Siriruk Pimmasarn, Pierre Ploton, Nophea Sasaki, Salvotore Virdis, Maxime Réjou-Méchain

Table S1. Lidar metrics (n = 21) and their descriptions

Performance comparisons of several LiDAR-derived metrics to infer AGB at 0.5-ha resolution. Metrics (1-17) were calculated directly from the LiDAR cloud dataset and metrics (18-21) were derived from the canopy height model (CHM), which itself derived from the LiDAR cloud data. LOOCV-RMSE is the back-transformed error of the LiDAR-AGB log-log model obtained through a leave-one-out scheme (see methods). The relative RMSE is the ratio of this LOOCV-RMSE to the mean of field AGB. From all the metric the mean top-of-canopy-height (TCH) derived from CHM was the best metric selected, highlighted row in table.

S.No.	*LiDAR metric*	*LOOCV-RMSE*	*Relative RMSE (in%)*
1	H_{10} *(10th Percentile)*	93.53	29.70
2	H_{25} *(25th Percentile)*	72.13	22.90
3	H_{50} *(50th Percentile)*	48.73	15.47
4	H_{75} *(75th Percentile)*	50.08	15.90
5	H_{95} *(95th percentile)*	67.78	21.52
6	H_{IQR} *(HIQR = Q75 - Q25)*	81.02	25.72
7	H_{mean}	47.16	14.97
8	H_{sqmean} *(quadratic mean)*	48.44	15.38
9	H_{cv} *coefficient of variation of all height*	94.79	30.10
10	Bin95 *(Percent of points within Q95)*	93.95	29.83
11	Bin75 *(Percent of points within Q75)*	96.51	30.64
12	Bin50 *(Percent of points within Q50)*	95.54	30.33
13	Bin25 *(Percent of points within Q25)*	95.51	30.32
14	Hperc10 *Percentage of height ranges in 0–10m*	91.76	29.13
15	Hperc20 *Percentage of height ranges in 0–20m*	74.45	23.64
16	Hperc30 *Percentage of height ranges in 0–30m*	74.98	23.81
17	Hperc40 *Percentage of height ranges in 0–40m*	89.75	28.50
18	TCH *(Mean of top of Canopy Height)*	45.2	14.35
19	CHM_H50	47.8	15.18
20	$CHMH_{relief}$ *(((mean - min) / (max – min))*	90.12	28.61

21	CHMSqMean	46.83	14.87

Table S2. Results from the model selection approach using TCH and any other of the additional LiDAR-based metrics described in Table S1 in a log-log linear model of the form $log\ (AGB) = a + b \times log\ (TCH) + c \times log\ (X)$, where X is the additional metric tested given in the table. LOOCV-RMSE is the back-transformed error of this model obtained through a leave-one-out scheme (see methods). The relative RMSE is the ratio of the LOOCV-RMSE to the mean of field AGB. Adding a second predictor did not reduce the relative LOOCV-RMSE by more than 1, so only TCH was selected as final predictor.

Log- Log Model	**LOOCV-RMSE RMSE**	**Relative RMSE Relative to mean AGB**
AGB~TCH	45.2	14.35%
AGB~ **TCH** + Bin 95	44.90	14.26%
AGB~ **TCH** + Bin 95+H10	43.86	13.96%
AGB~ **TCH** + Bin 95+H10+Hperc40	45.11	14.32%

Table S3: Landsat Time-series data used for the study with corresponding validation score

S.No	Landsat Mission	Sensor	Date of collection	Validation Score
1	Landsat 1-3	MSS	19/12/1972	94.12
2	Landsat 1-3	MSS	6/1/1973	90.69
3	Landsat 1-3	MSS	13/12/1975	92.65
4	Landsat 1-3	MSS	18/01/1976	94.12
5	Landsat 1-3	MSS	18/11/1978	94.61
6	Landsat 1-3	MSS	1/12/1979	96.57
7	Landsat 1-3	MSS	13/01/1982	95.1
8	Landsat 4-5	TM	9/12/1987	94.61
9	Landsat 4-5	TM	11/12/1988	96.57
10	Landsat 4-5	TM	13/02/1989	96.08
11	Landsat 4-5	TM	5/4/1990	98.53
12	Landsat 4-5	TM	2/11/1991	97.06
13	Landsat 4-5	TM	18/03/1992	95.1
14	Landsat 4-5	TM	23/11/1993	96.08
15	Landsat 4-5	TM	28/12/1994	94.12
16	Landsat 4-5	TM	20/03/1996	96.08
17	Landsat 4-5	TM	20/12/1997	91.67
18	Landsat 4-5	TM	23/12/1998	92.65
19	Landsat 4-5	TM	26/12/1999	96.08
20	Landsat 4-5	TM	12/12/2000	95.1
21	Landsat 4-5	TM	2/3/2001	94.61
22	Landsat 4-5	TM	24/01/2002	97.06
23	Landsat 4-5	TM	21/11/2004	97.55
24	Landsat 4-5	TM	13/03/2005	98.04
25	Landsat 4-5	TM	13/12/2006	94.61
26	Landsat 4-5	TM	30/01/2007	95.1
27	Landsat 4-5	TM	18/12/2008	94.12
28	Landsat 4-5	TM	19/11/2009	92.65
29	Landsat 4-5	TM	25/01/2011	95.59
30	Landsat 8	OLI & TIRS	30/11/2013	89.71
31	Landsat 8	OLI & TIRS	19/12/2014	93.14
32	Landsat 8	OLI & TIRS	2/4/2015	91.67
33	Landsat 8	OLI & TIRS	11/3/2016	95.1
34	Landsat 8	OLI & TIRS	25/01/2017	96.57

Figures

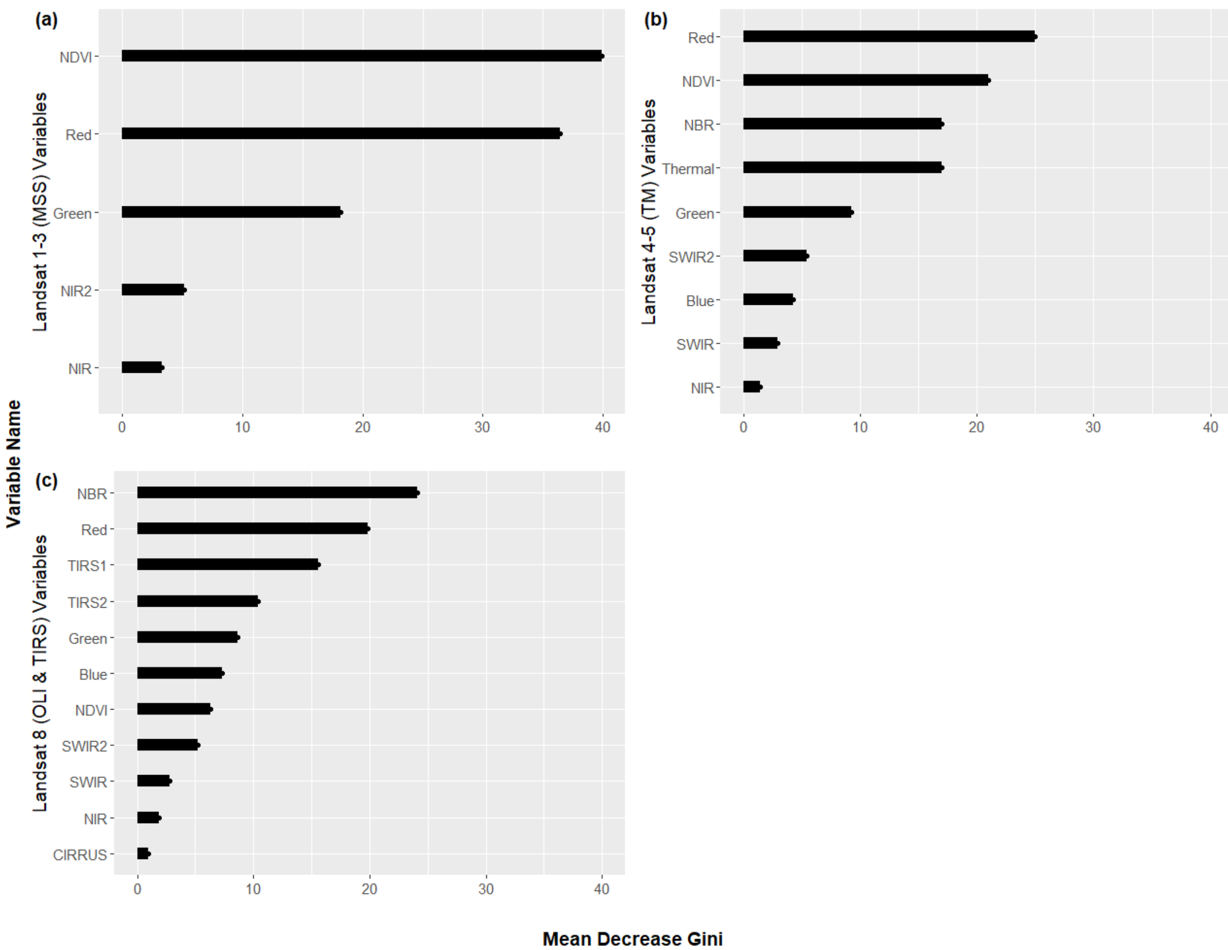

Fig S1: Random Forest results showing the average variable importance in each Landsat sensors used for classification (a) Average variable importance for Landsat 1-3 (MSS) sensor images (1972–1983) (b) Average variable importance for Landsat 4-5 (TM) sensor images (1984–2011) (c) Average variable importance for Landsat 8 (OLI & TIRS) sensor images (2013-2017)

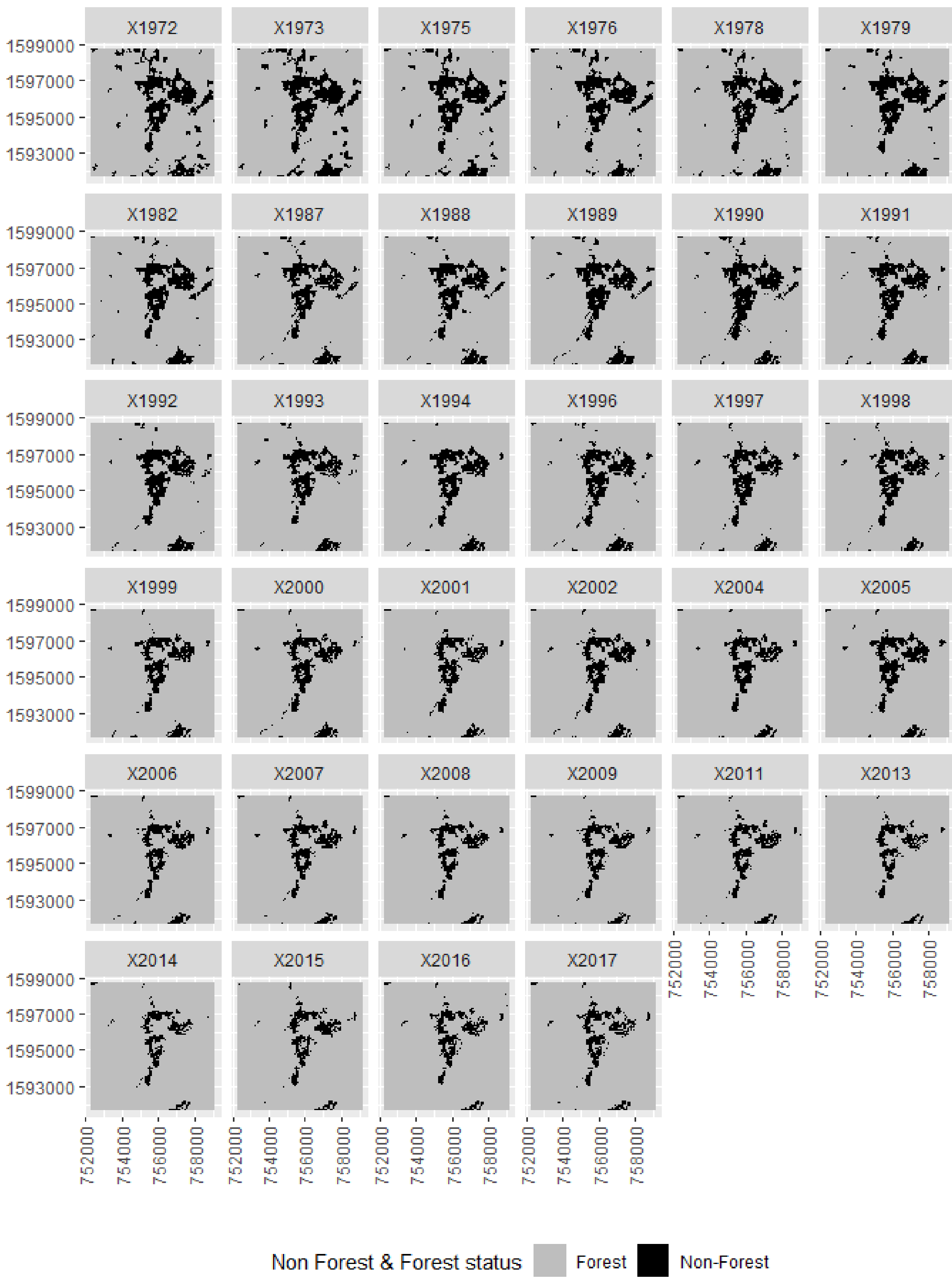

Fig S2: Non-Forest and Forest status across period (1972-2017)

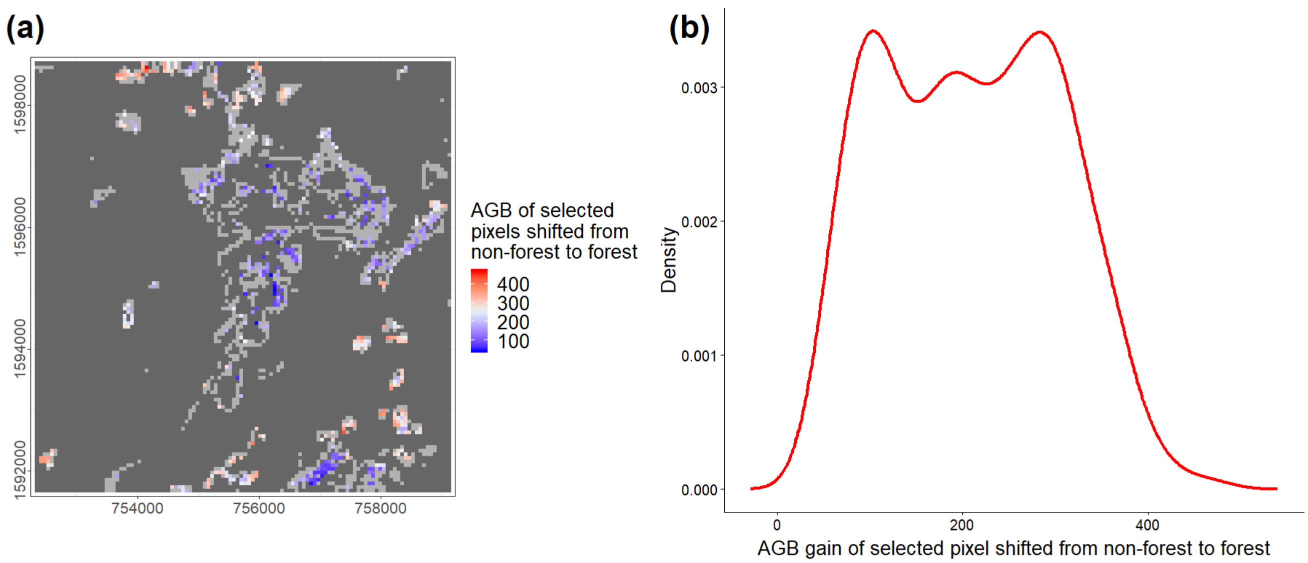

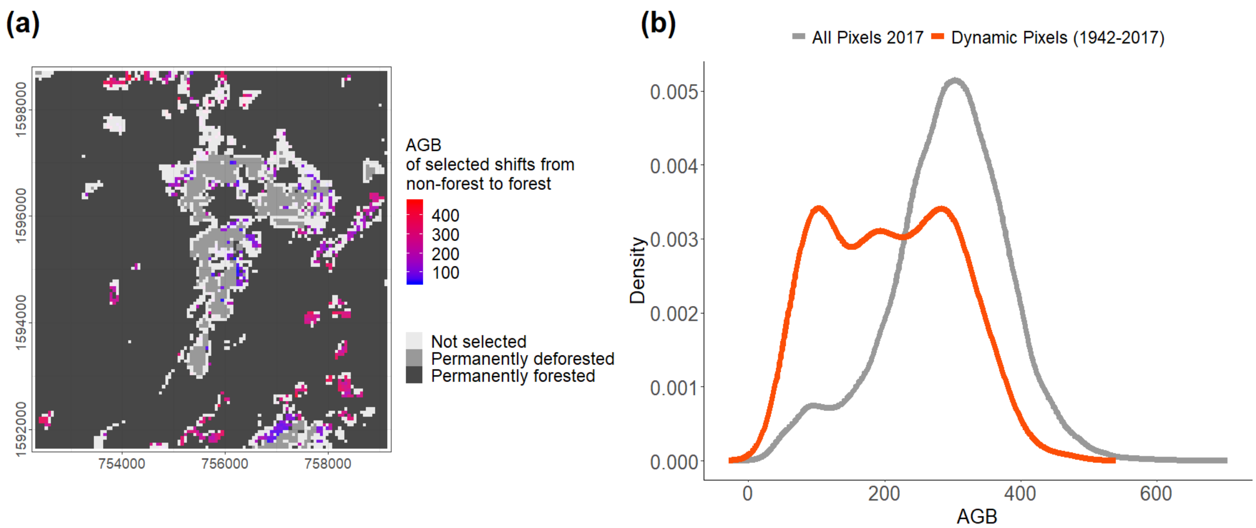

Fig S3~~2~~: AGB recovery of the pixels that experienced a single shift from Non-Forest to Forest. (a)- Map showing spatialized single shifts from non-forests to forests with the corresponding AGB gain in 2017 as predicted by our LiDAR AGB map (Fig. 3a). ~~-~~The shade gradient represents pixels that did not experience any shift (permanently forested or permanently deforested) and pixels that experienced a shift but that did not pass our quality procedure during the study period (Not selected) (b)- Density distribution of pixels with AGB gain which experiences single shifts over the landscape during the study period compared with the density distribution of predicted AGB over full landscape 2017 (Fig. 3b)~~.~~

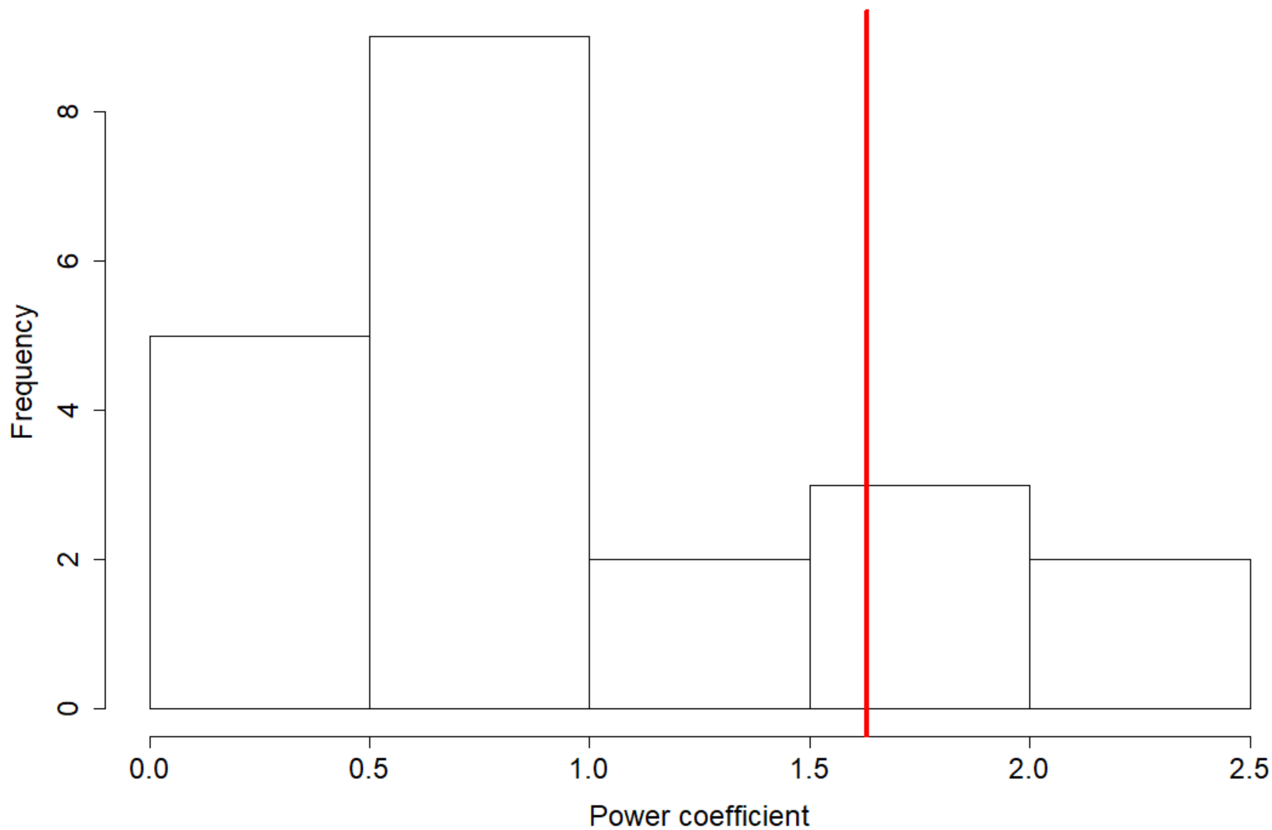

Fig S4~~3~~: Distribution of the power coefficients obtained from site-specific power models fitted on AGB recovery versus forest age in 21 sites studied by Poorter et al. (2016) and in our site (red line). We only considered the sites having a minimum of 10 observations and that were younger than 45 years old. We excluded 7 sites matching those rules as they exhibited dubious patterns of carbon recovery through time that cannot be captured by a power model (sites Eastern Pará 2, El Carite, Mata Seca, Patos, San Carlos, Yucatán, Zona Norte).

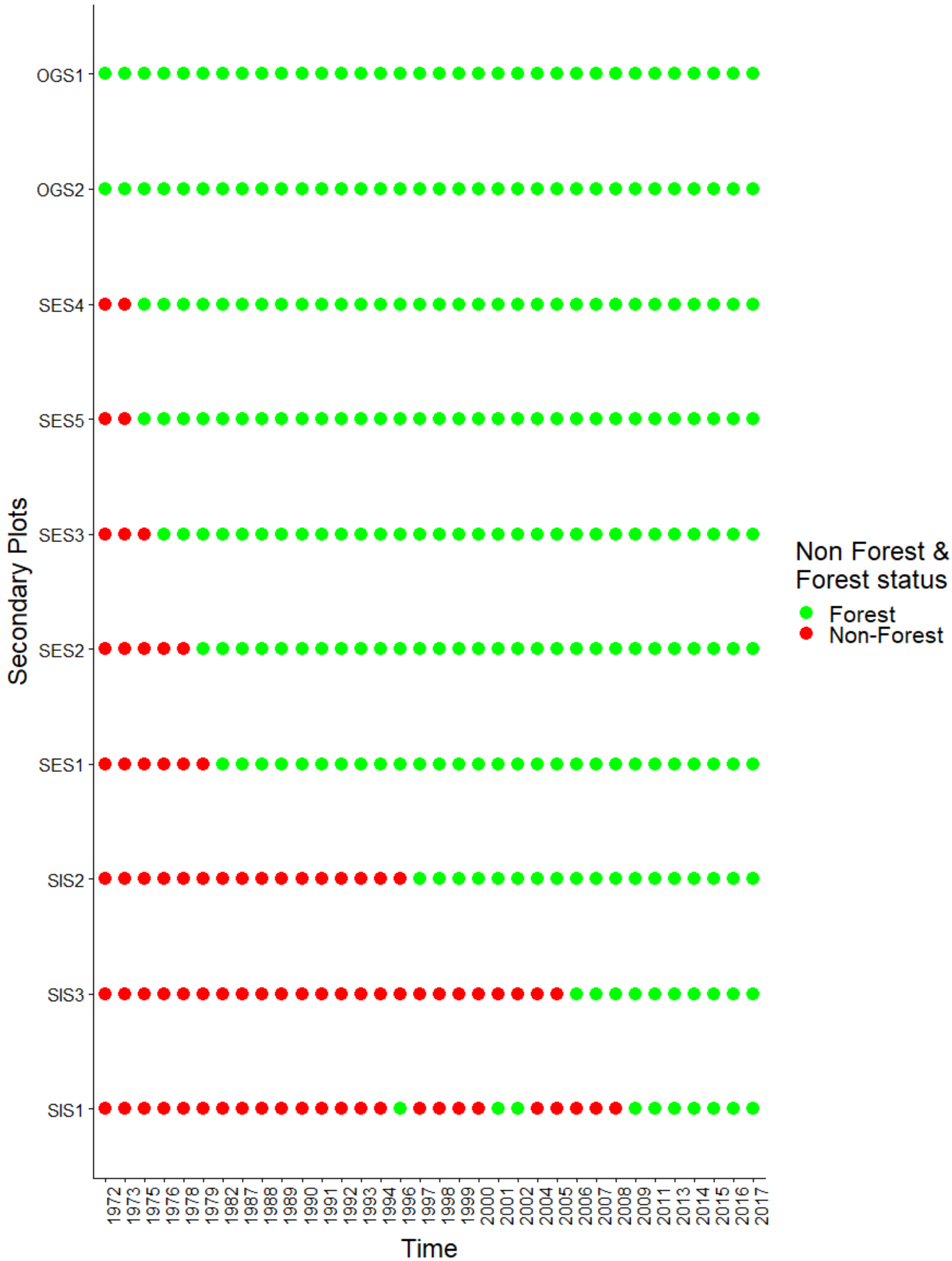

Fig S5. Non-forest (red) to forest (green) status during the 1972-2017 period in 10 field plots belonging to different successional stages as estimated from our forest classification approach. We did not represent here the subplots belonging to the Mo Singto plot as they all were in a forested status during the whole study period.